PECS Radar Remote Sensing Course

ESA – UNIVERSITY OF MARIBOR

10th September 2015 – Maribor

Advanced topics

Dr. Francisco López-Dekker (DLR, German Aerospace Center)

esa

DLR Deutsches Zentrum für Luft- und Raumfahrt e.V. in der Helmholtz-Gemeinschaft

QUILL (National Reconaissence Office)

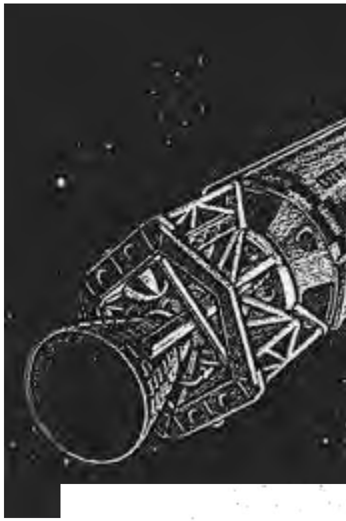

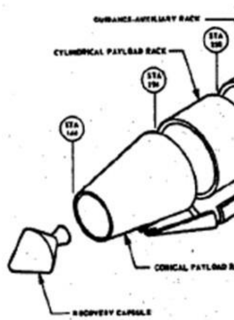

Figure 4.
Source: Lock

Parameter	Value
Launch	Dec 21st, 1964
	GHz (X-band)
	m× 4.6 m
	vnlink + Tape
	(azimuth)
	5-8735 Hz
	km
	ft (24 m)
	W
	6 us (16 MHz)
	deg

Spaceborne SAR Missions since 1978

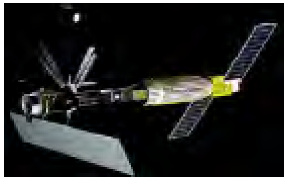

SEASAT

NASA/JPL (USA)

L-Band, 1978

ERS-1/2

European Space Agency (ESA)

C-Band,
1991-2000 & 1995-2011

J-ERS-1

Japanese Space Agency (NASDA)

L-Band, 1992-1998

SIR-C/X-SAR

NASA/JPL, L- and C-Band (quad)

DLR / ASI, X-band

April and October 1994

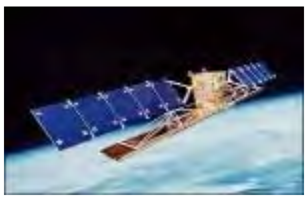

RADARSAT-1

Canadian Space Agency (CSA)

C-Band, 1995-today

SRTM

NASA/JPL (C-Band), DLR/ASI (X-Band)

February 2000

ENVISAT / ASAR

European Space Agency (ESA)

C-Band (dual), 2002-today

ALOS / PALSAR

Japanese Space Agency (JAXA)

L-Band (quad), 2005-2011

SAR Lupe

BWB Germany

X-Band, 2006

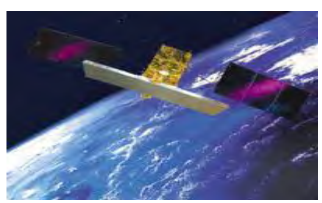

CosmoSkymed

ASI / Alenia

X-Band (dual), 2007

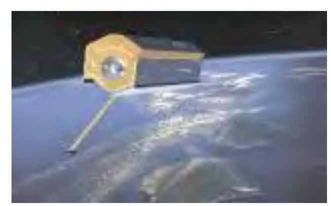

TerraSAR-X

German Aerospace Center (DLR) / Astrium

X-Band (quad), 2007

RADARSAT-2

Canadian Space Agency (CSA)

C-Band (quad), 2007

First Civilian SAR Satellite: Seasat (1978)

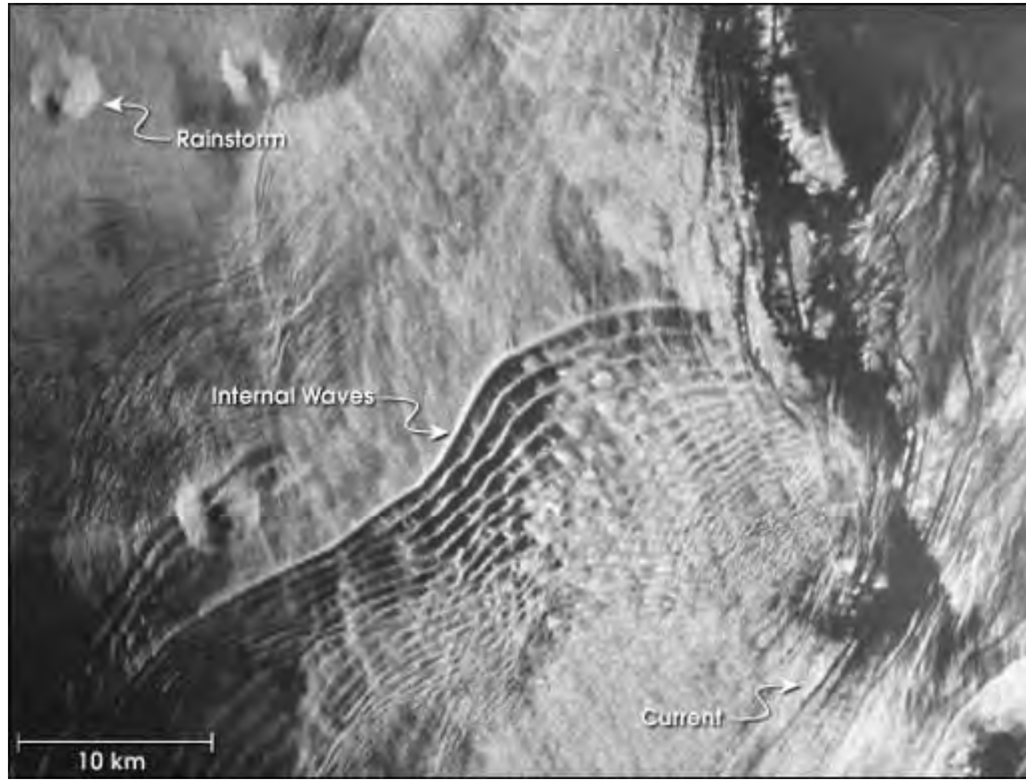

Launch	June 26, 1978	Wavelength	0,235 m
Altitude	~780 km	Bandwidth	19 MHz
Weight	2300 kg	Antenna Size	10,74 m x 2,16 m
Incident Angle	~ 23°		
Swath Width	100 km	Resolution	25 m x 25 m

RADARSAT-2 Imaging Modes

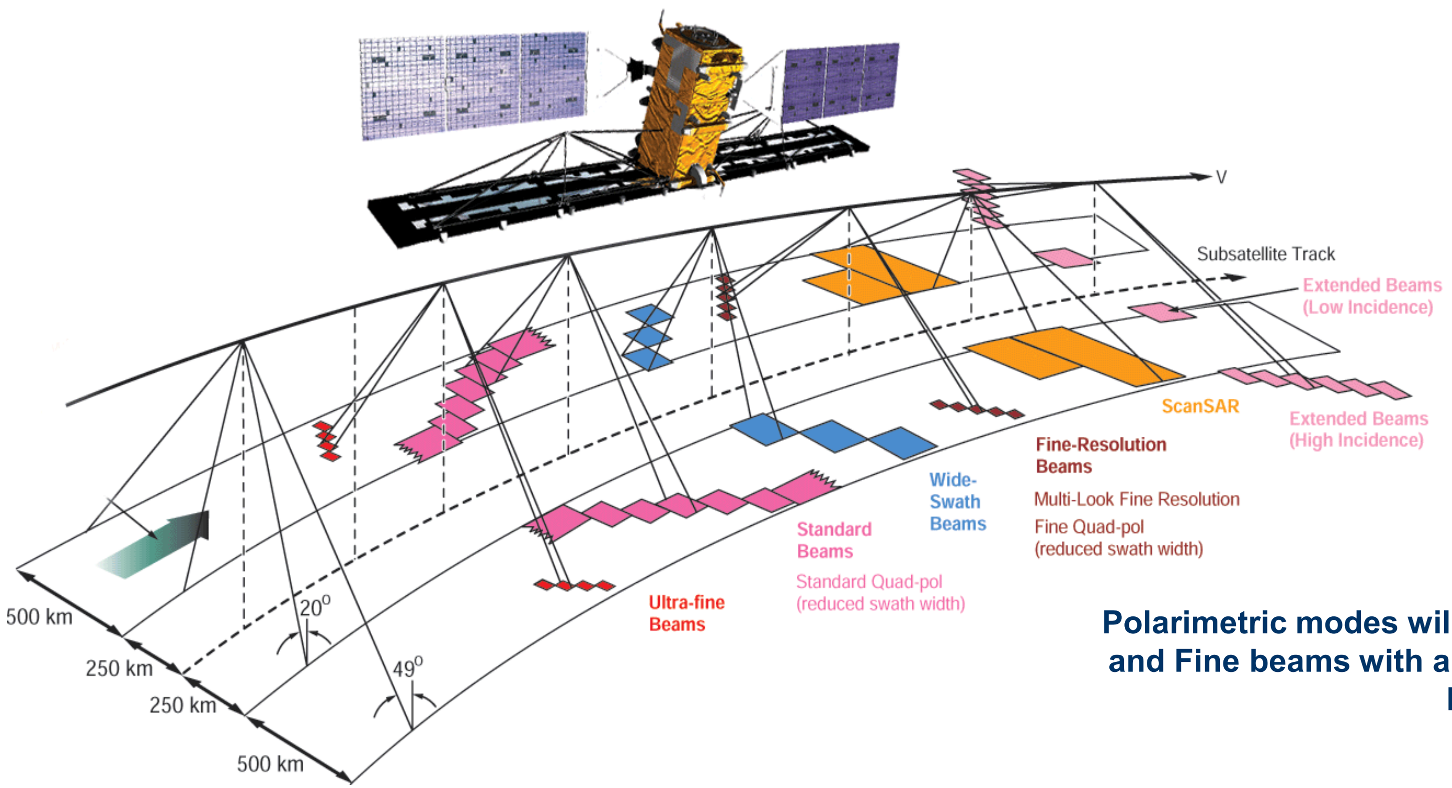

Polarimetric modes will be available on Standard and Fine beams with a limited swath width of 25 km.

All modes will be available in selective single or dual polarization.

All modes will be available on either side of the satellite.

MACDONALD DETTWILER®

TerraSAR-X Satellite

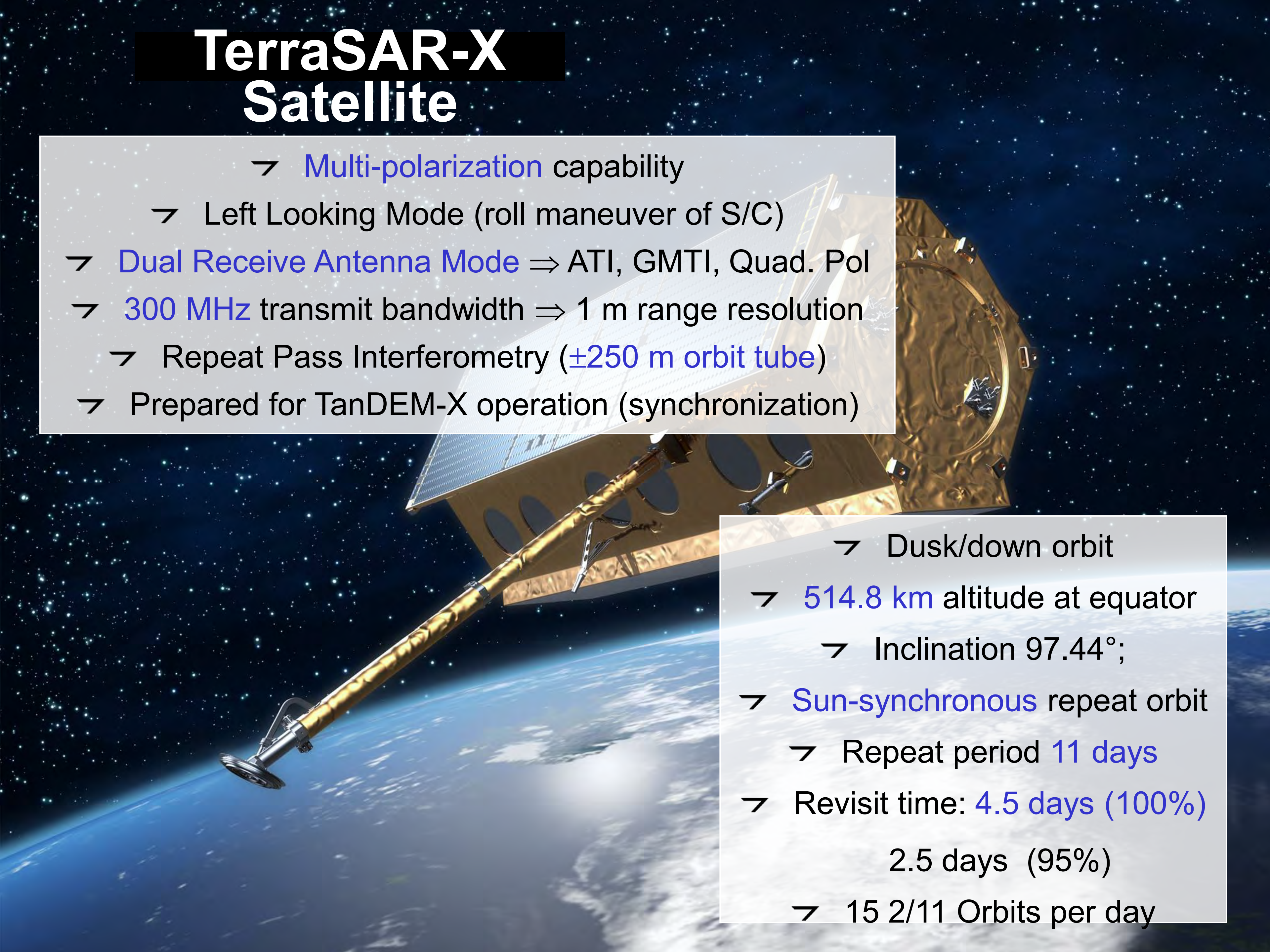

- Multi-polarization capability
- Left Looking Mode (roll maneuver of S/C)
- Dual Receive Antenna Mode ⇒ ATI, GMTI, Quad. Pol
- 300 MHz transmit bandwidth ⇒ 1 m range resolution
- Repeat Pass Interferometry (±250 m orbit tube)
- Prepared for TanDEM-X operation (synchronization)

- Dusk/down orbit
- 514.8 km altitude at equator
- Inclination 97.44°;
- Sun-synchronous repeat orbit
- Repeat period 11 days
- Revisit time: 4.5 days (100%)
  2.5 days (95%)
- 15 2/11 Orbits per day

TanDEM-X

TerraSAR-X ad-on for

Digital Elevation Measurments

- *Acquisition of a global DEM according to HRTI-3 standard*
- *Generation of local DEMs with HRTI-4 like quality*
- *Demonstration of innovative techniques (formation flying, bistatic acquisiton, Pol-InSAR)*

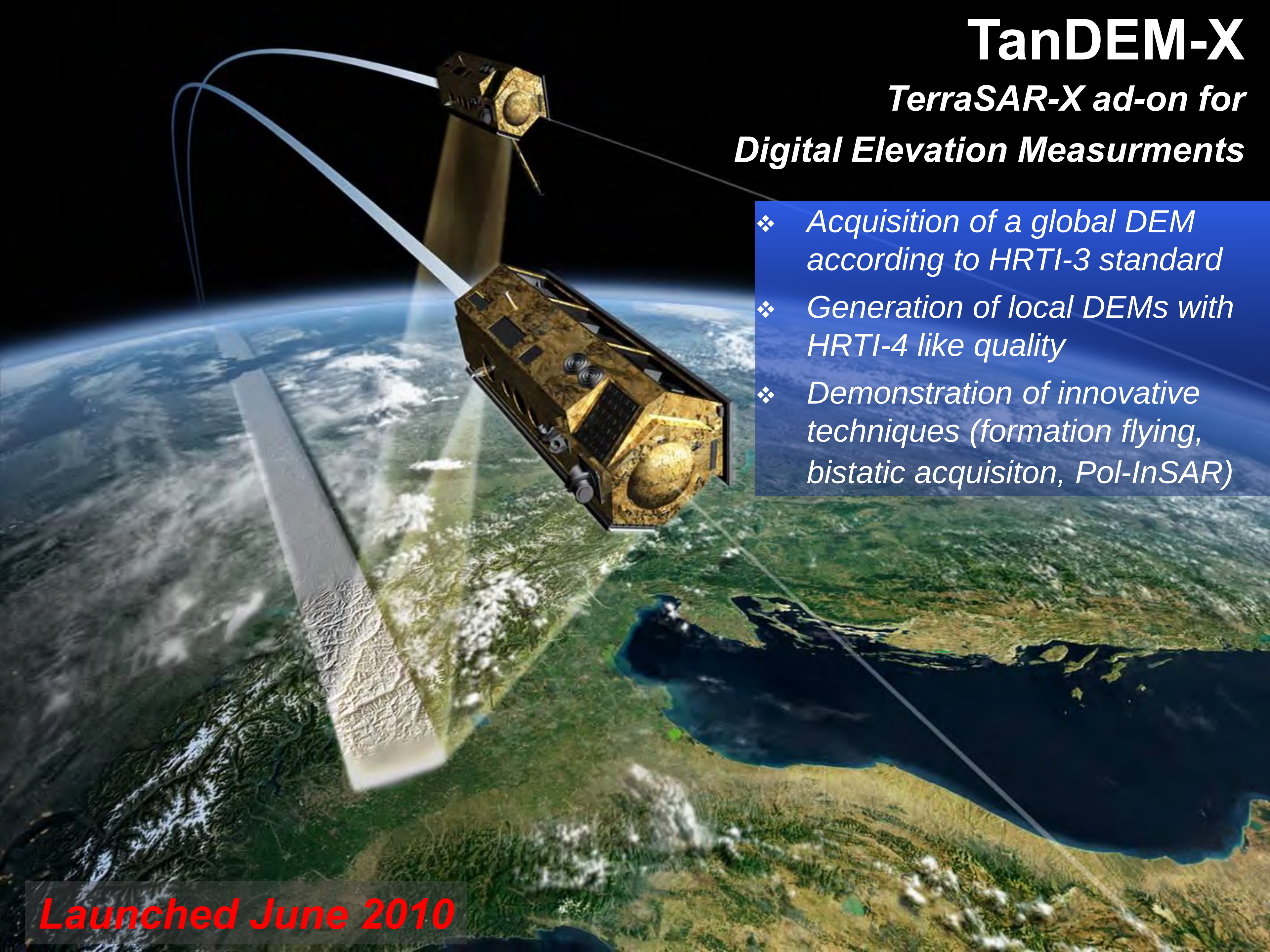

Launched June 2010

TanDEM-X Orbit Configuration

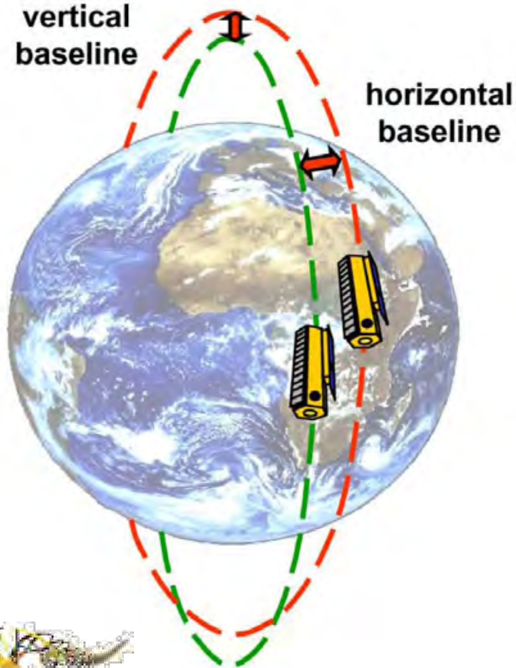

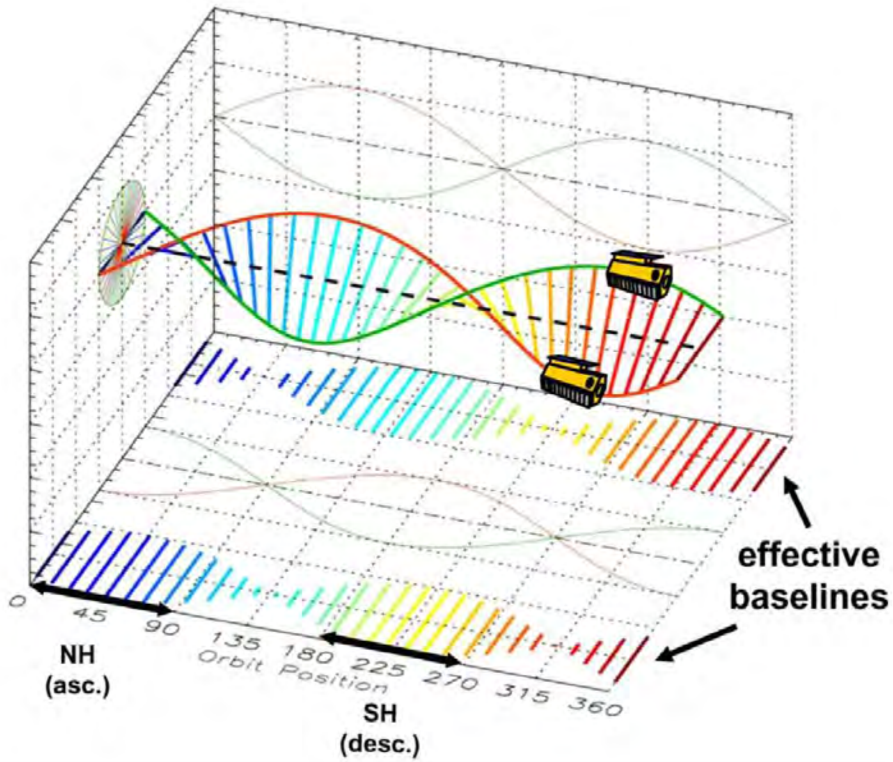

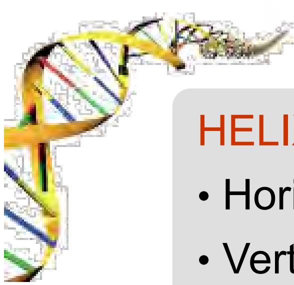

HELIX satellite formation allows safe operation

- Horizontal cross-track separation at equator by different ascending nodes
- Vertical separation at poles by orbits with different eccentricity vectors
- No crossing of single orbits
- Variation of baselines in cross-track and along-track easily achievable

NGA (NIMA) Standards for Digital Elevation Models

	Spatial Resolution	Absolute Vertical Accuracy (90%)	Relative Vertical Accuracy (point-to-point in 1° cell, 90%)
DTED-1	90 m x 90 m	< 30 m	< 20 m
DTED-2	30 m x 30 m	< 18 m	< 12 m
HRTI-3	12 m x 12 m	< 10 m	< 2 m
HRTI-4	6 m x 6 m	< 5 m	< 0.8 m

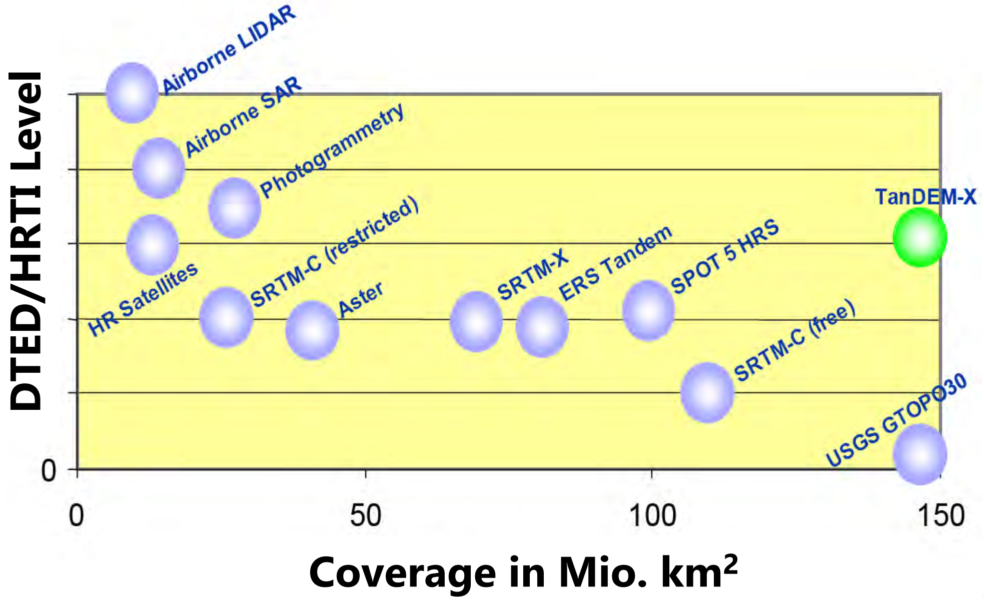

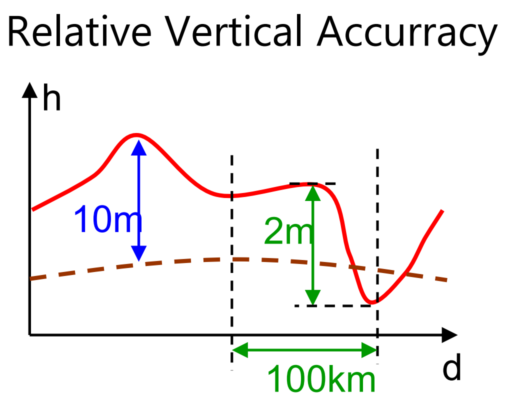

NGA (NIMA) Standards for Digital Elevation Models

	Spatial Resolution	Absolute Vertical Accuracy (90%)	Relative Vertical Accuracy (point-to-point in 1° cell, 90%)
DTED-1	90 m x 90 m	< 30 m	< 20 m
DTED-2	30 m x 30 m	< 18 m	< 12 m
HRTI-3	12 m x 12 m	< 10 m	< 2 m
HRTI-4	6 m x 6 m	< 5 m	< 0.8 m

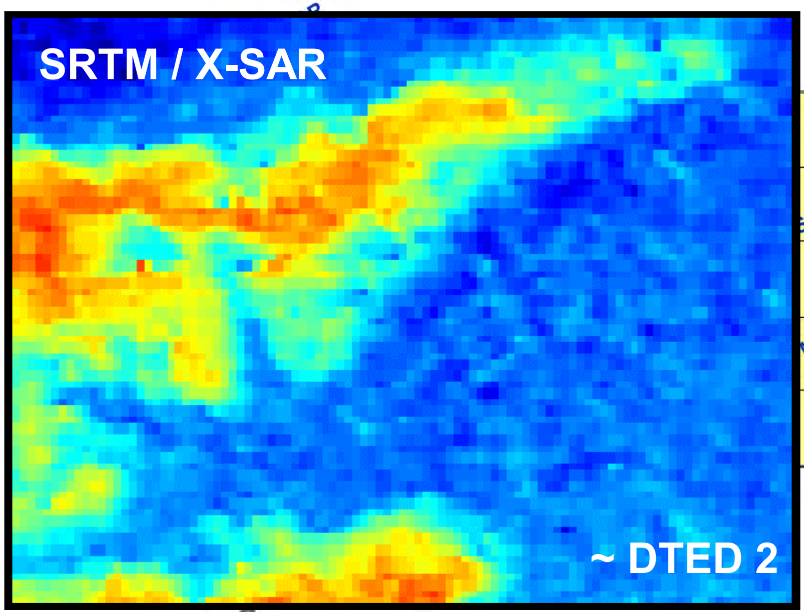

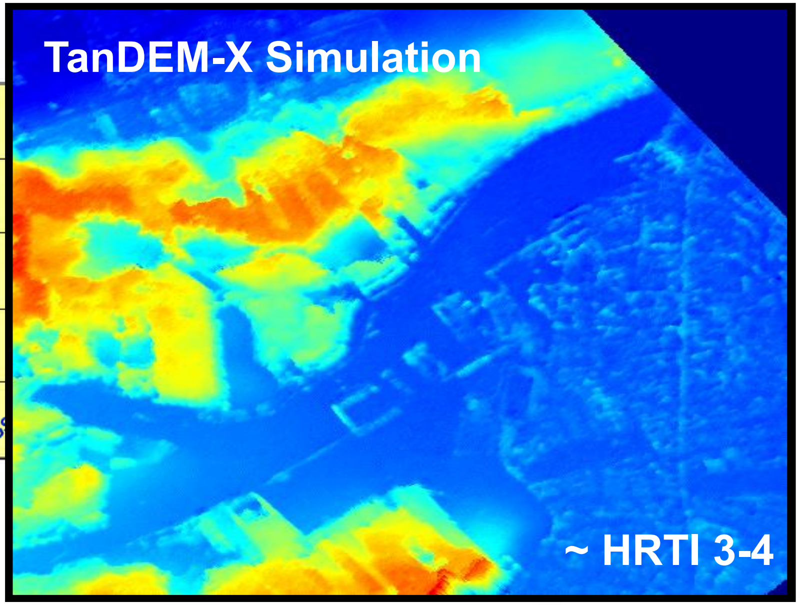

1 SRTM 90m pixel = 7.52 TanDEM-X pixels (1D)
56 times finer (2D)

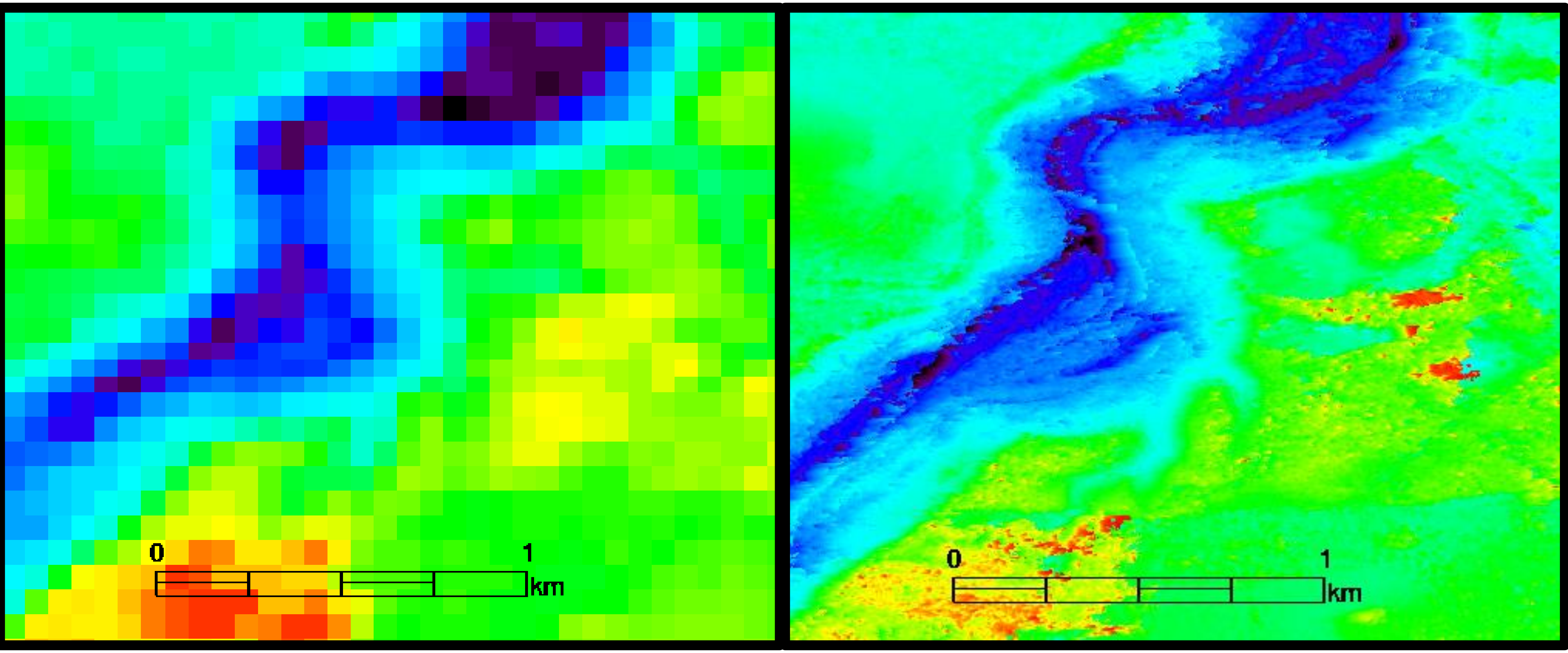

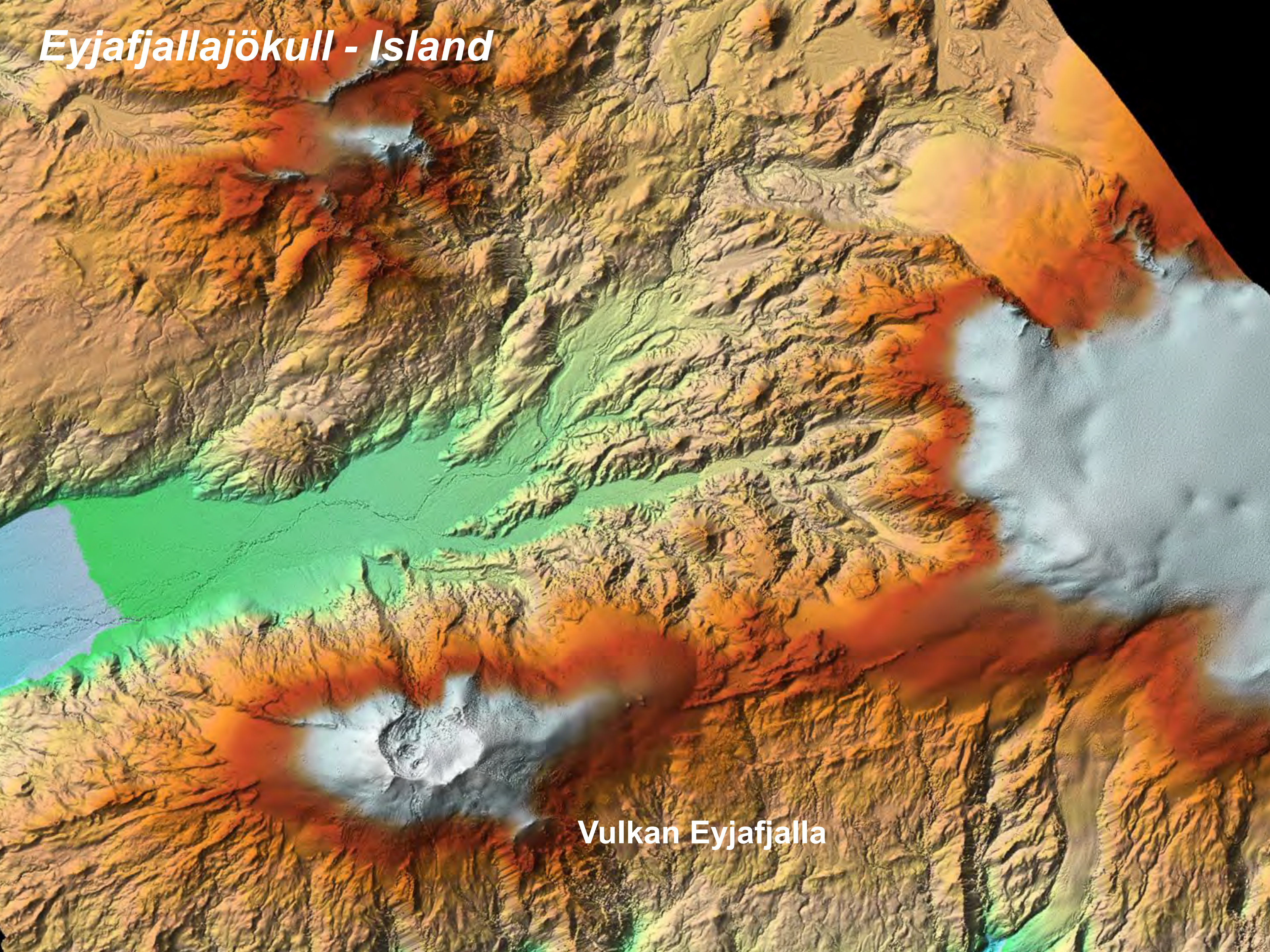
Eyjafjallajökull - Island
Vulkan Eyjafjalla

Future Developments: **Bistatic SAR**

Bistatic SAR Imaging

Enhanced Observation Space

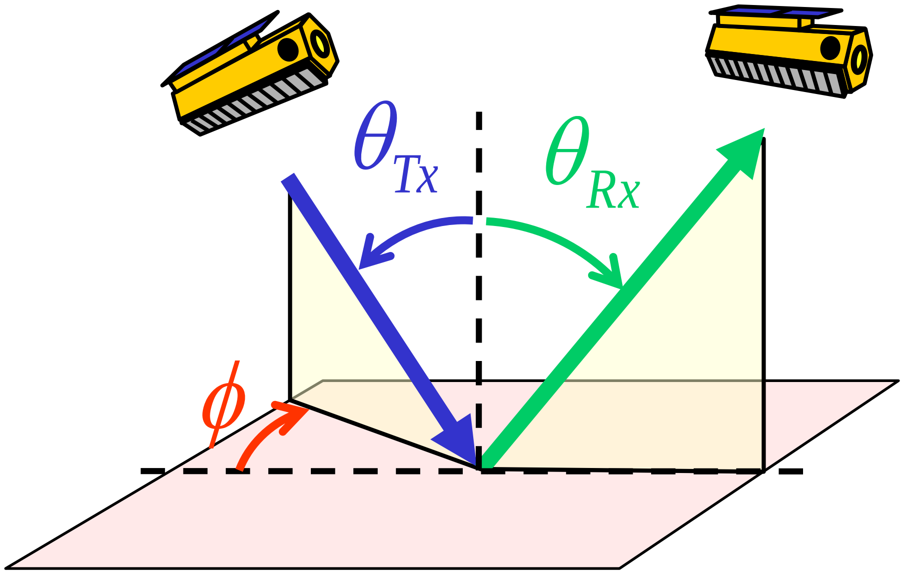

- Improved detection, segmentation and classification (bistatic scattering)
- New image and object parameters (bistatic Doppler, multiple shadows, …)

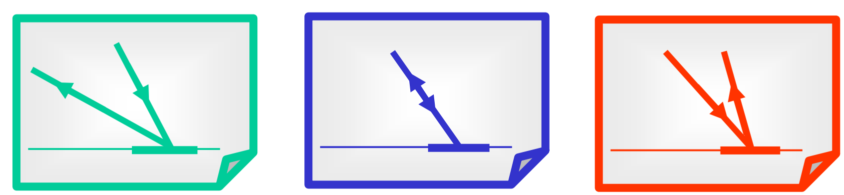

Hybrid Bistatic Radar Experiment with Satellite and Aircraft

- First hybrid X-band experiment worldwide
- Kaufbeuren, 5 November 2007
- TerraSAR-X transmits (Spotlight-Mode)
- F-SAR (airplane) receives (2 channels)

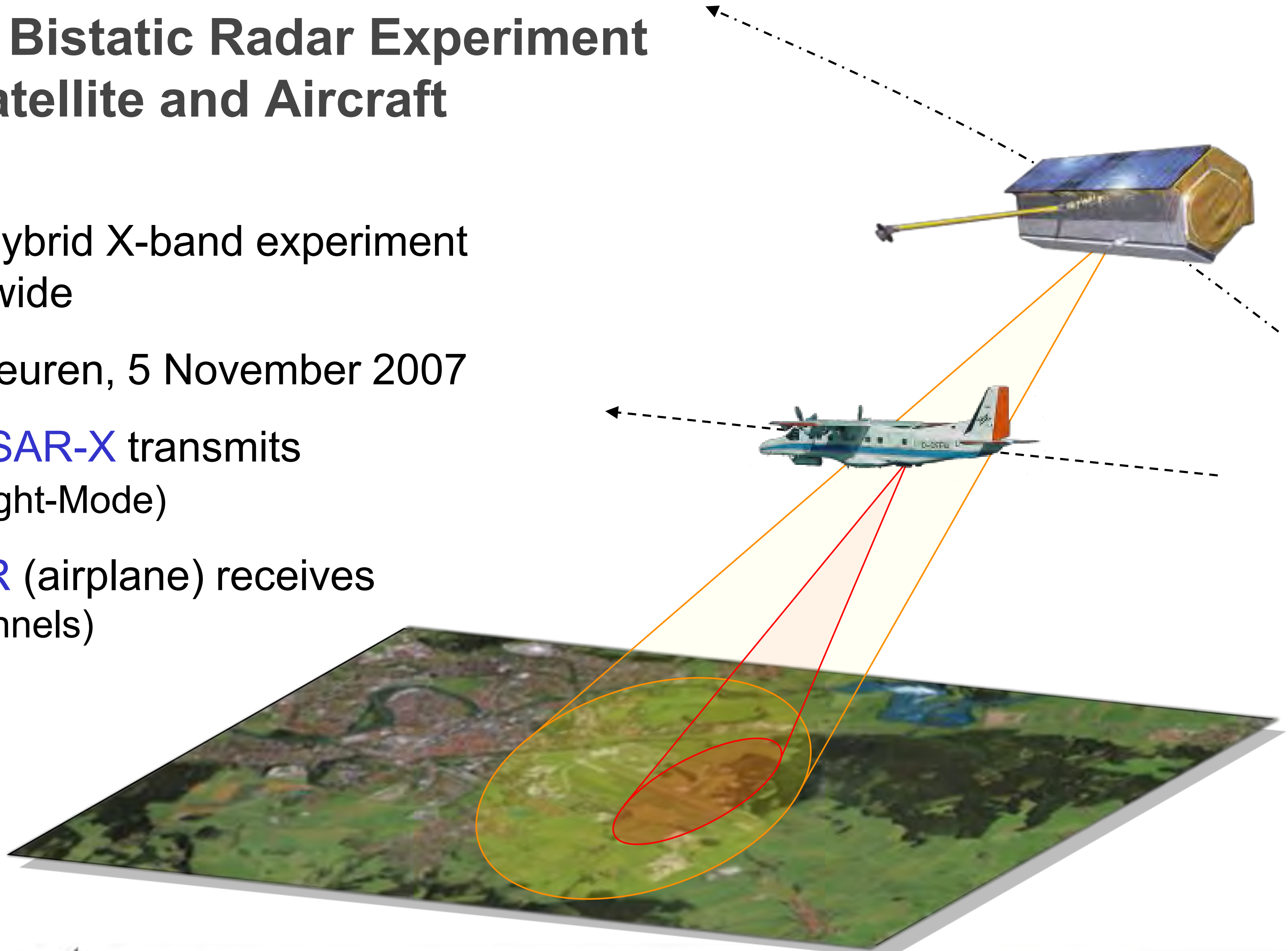

Hybrid Bistatic Experiment: Bistatic Image

- Bandwidth: 100 MHz
- Synchronization via direct signal and point target response
- Coherent Integration: 2.77 s
- Processing via bistatic backprojection algorithm

esa
DLR Deutsches Zentrum für Luft- und Raumfahrt e.V. in der Helmholtz-Gemeinschaft

Hybrid Bistatic Experiment: Bistatic Image

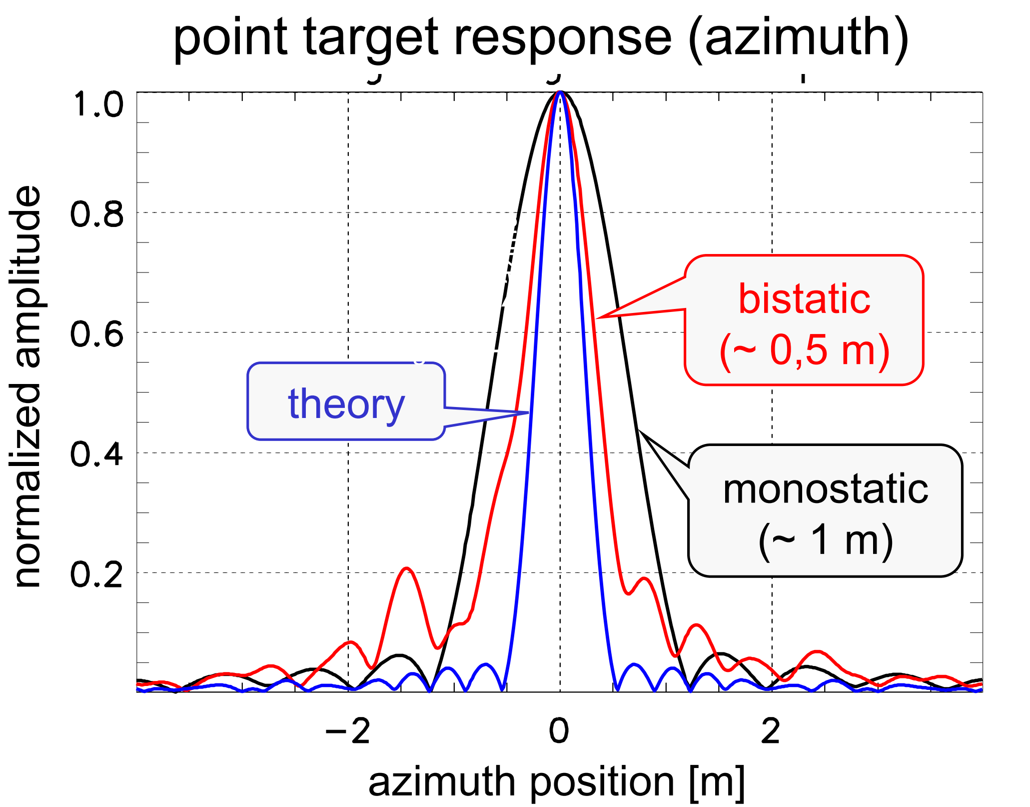

X-band Transponder

Hybrid Bistatic Experiment: Bistatic Image

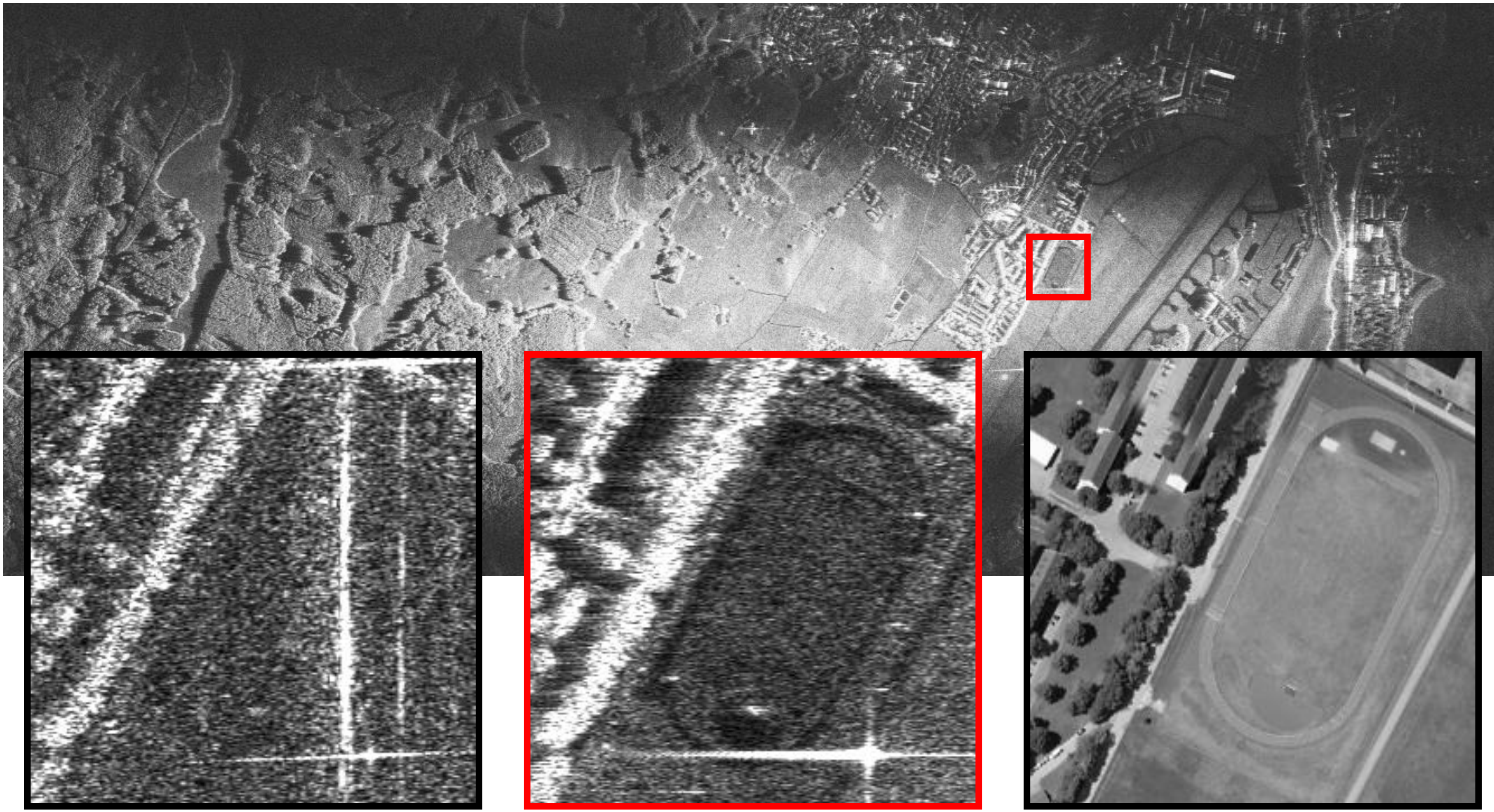

monostatic | bistatic | optic

Hybrid Bistatic Experiment: Bistatic Image

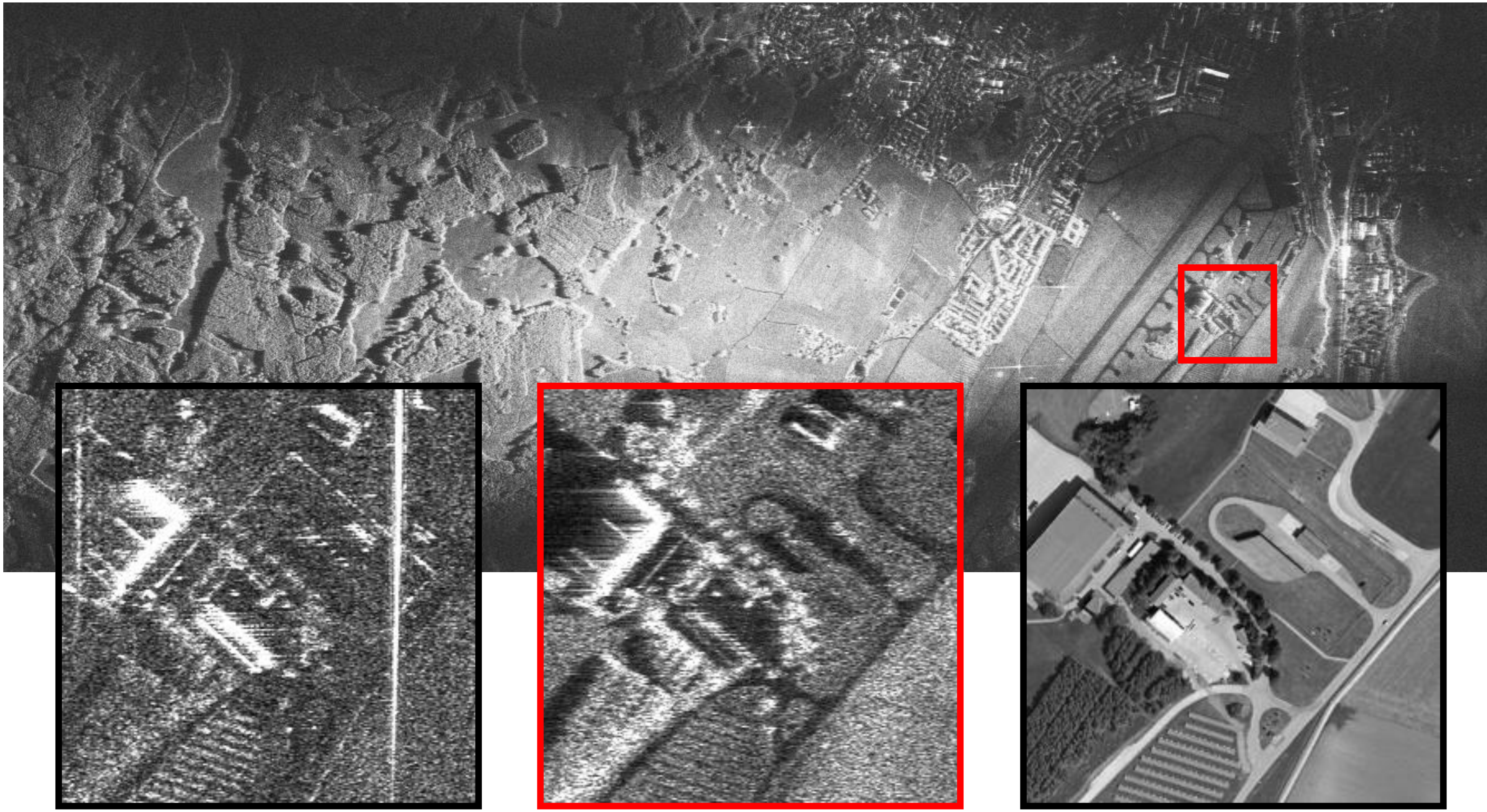

monostatic | bistatic | optic

Future Developments:

SAR Tomography

SAR Tomography

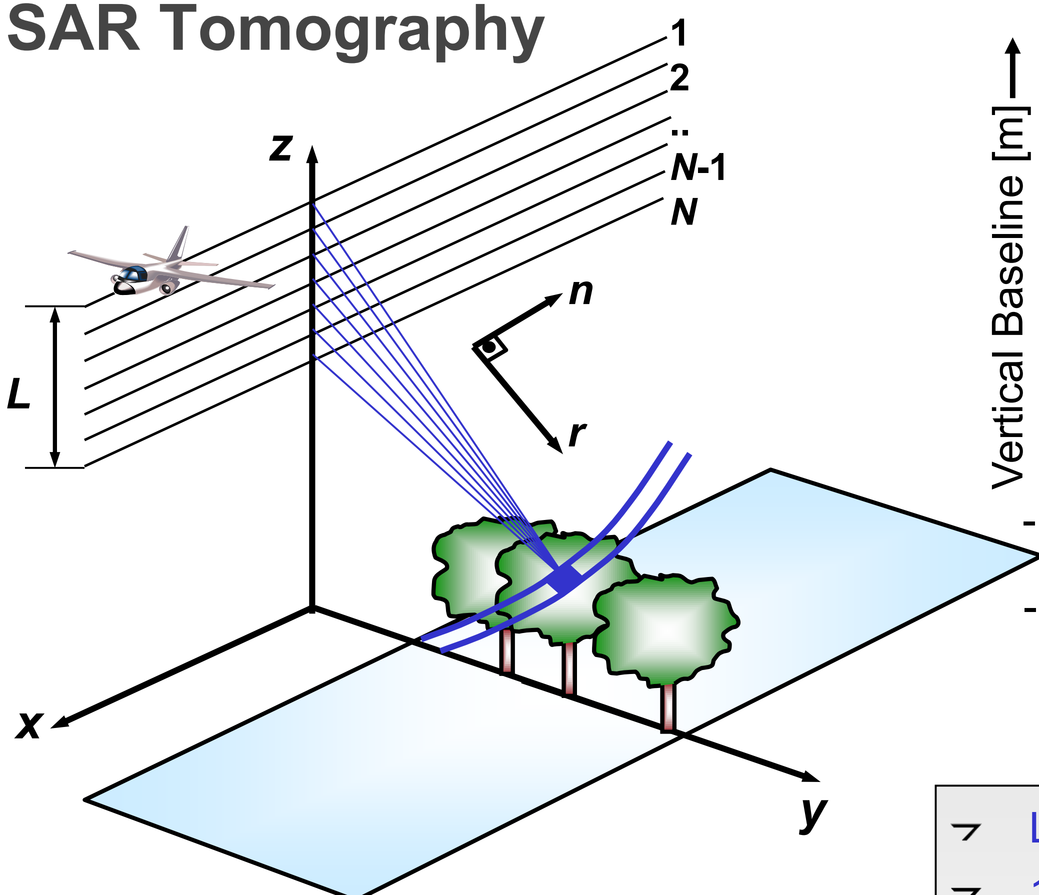

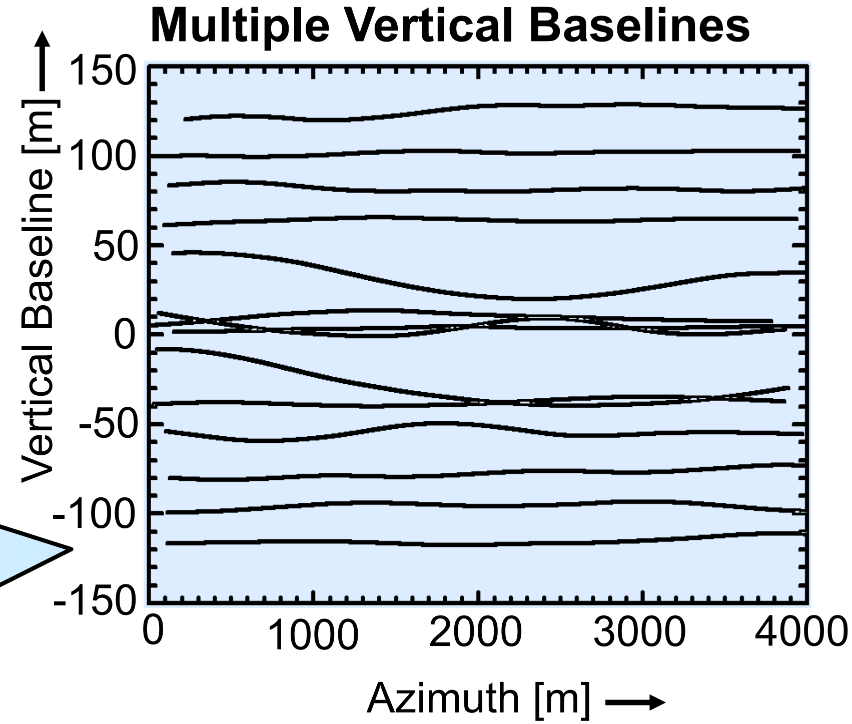

- 3D focusing for discrimination of targets in height
- Volumetric imaging
- Layover solution

- L-Band, 3000 m altitude
- 14 parallel tracks, 20 m distance between
- 240 m total baseline
- 3 m height resolution
- 3.5 hours flight time, 360 MByte/km

SAR Tomography: Experiment with E-SAR

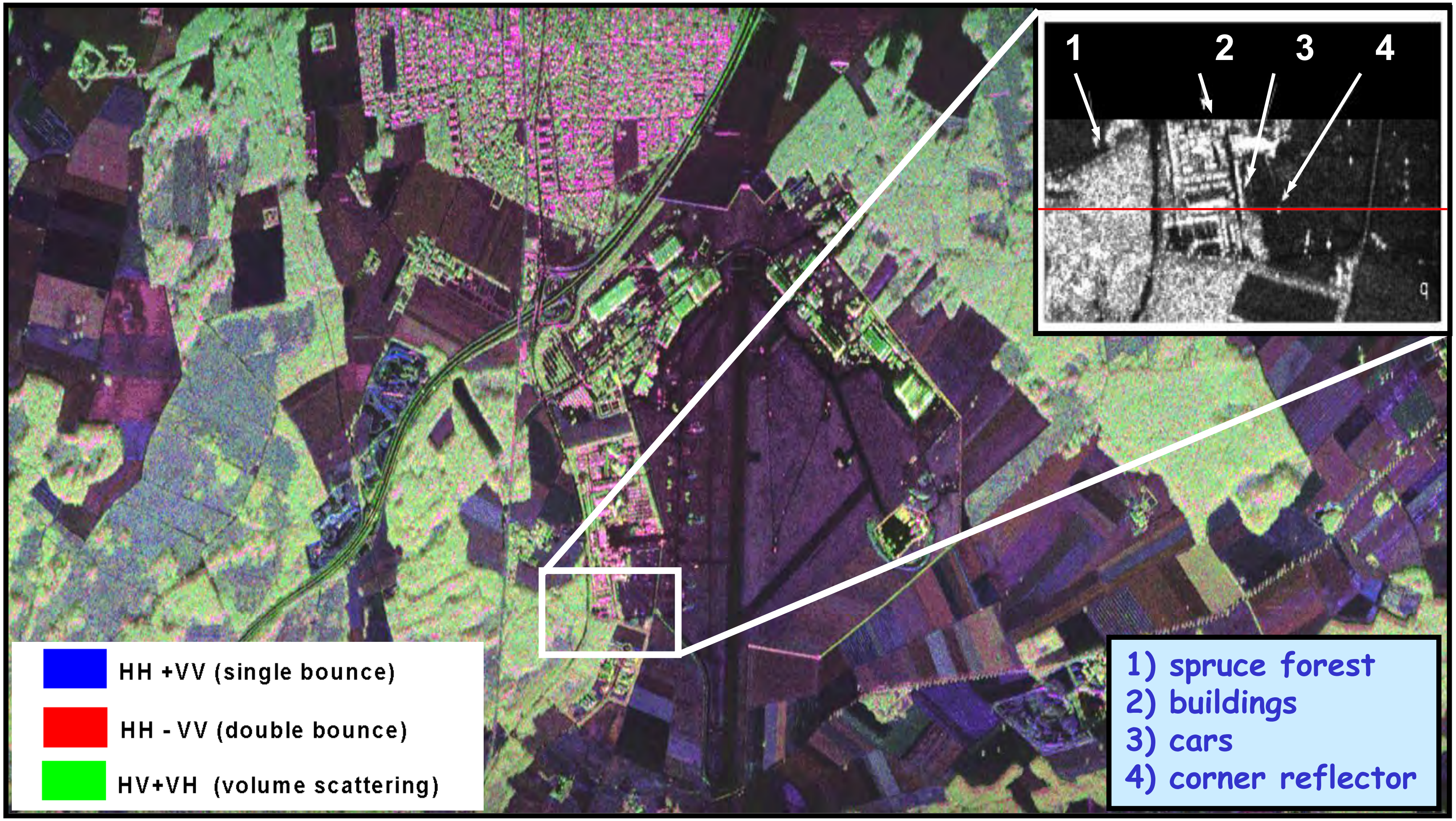

Deutsches Zentrum für Luft- und Raumfahrt e.V. in der Helmholtz-Gemeinschaft

First Demonstration of Airborne SAR Tomography [1)]

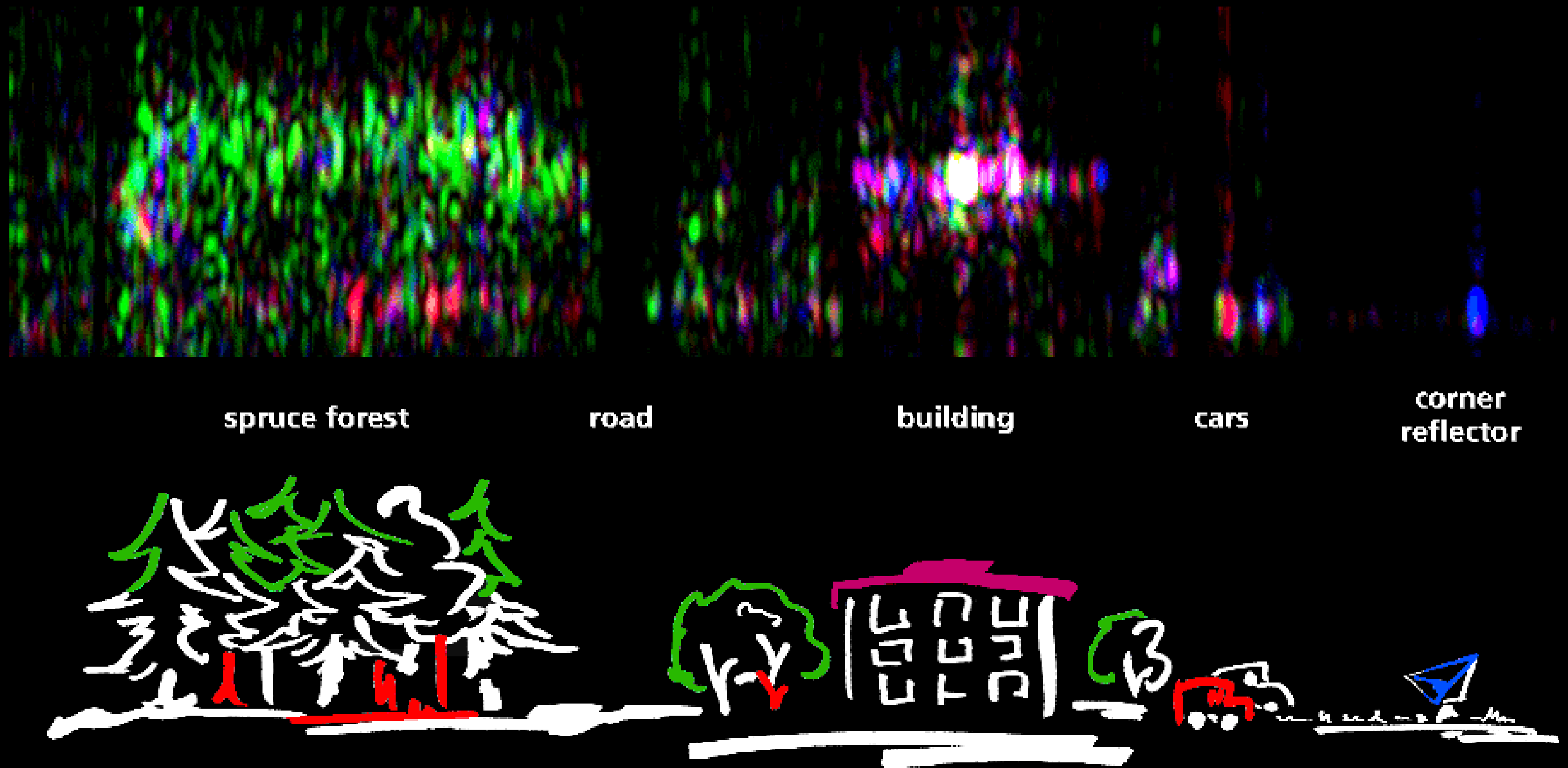

Airborne Polarimetric SAR Tomography

Upper image: Polarimetric color composite (L-band) of a tomographic slice in the height/azimuth-direction

HH+VV, HH-VV, 2*HV

Lower image: Schematic view of the imaged area

[1)] A. Reigber, A. Moreira, "First Demonstration of Airborne SAR Tomography using Multibaseline L-Band Data", IEEE TGRS, 2000

Measurement of 3D Structures: Tomography

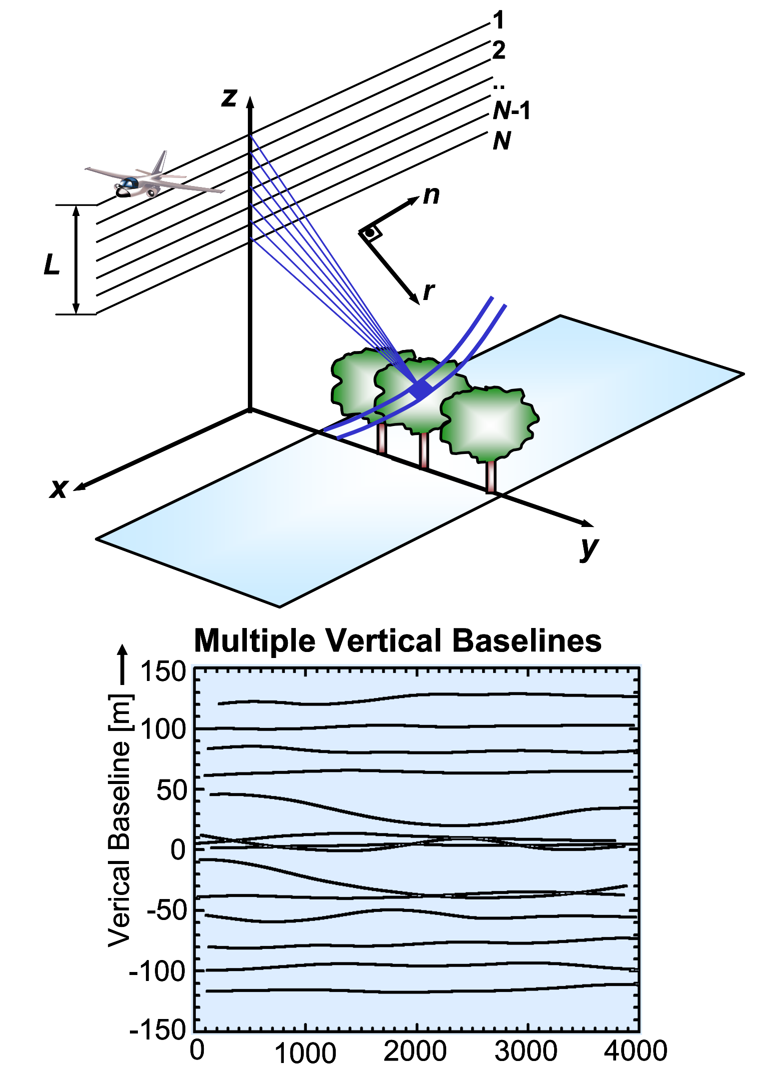

(Courtesy of A. Reigber)

Frequency Dependent Depth of Penetration

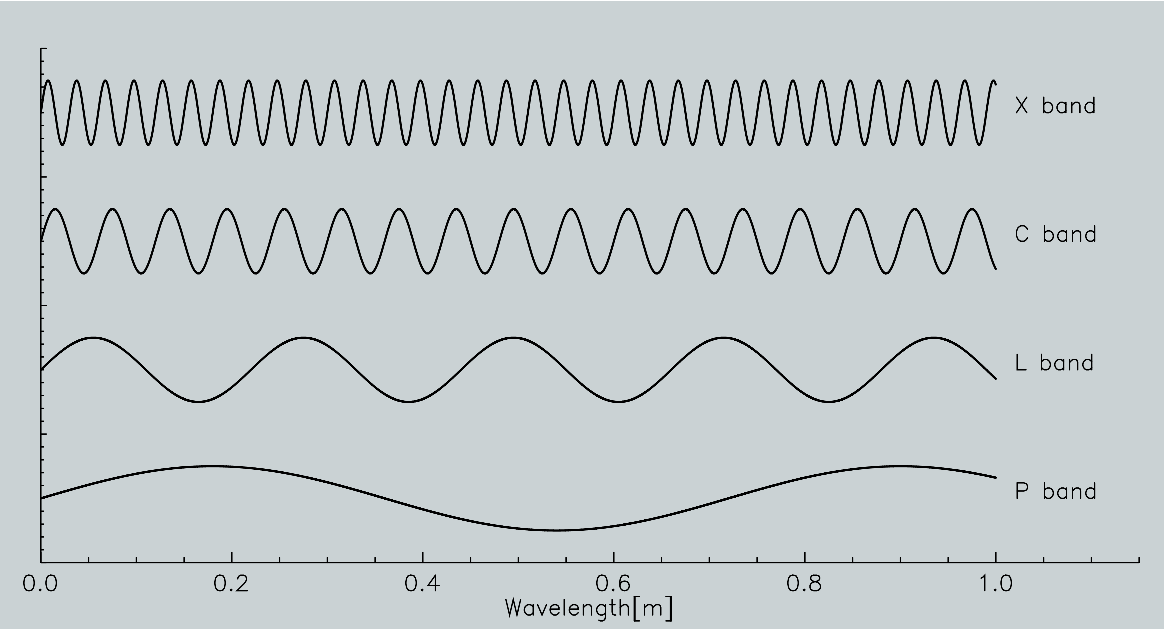

- Dependent on wavelength
- Different sensitivity on scatterer dimension
- Highest Backscatter for dimensions similar to wavelength

Wavelength		Main Scatterer
X Band	3 cm	Leaves, Twigs
C Band	6 cm	Leaves, Twigs, small Branches
L Band	22 cm	Branches, stem
P Band	76 cm	large Branches, stem

Penetration in Vegetation

Increases with wavelength

Future Developments:
Circular SAR

Circular Synthetic Aperture Radar (CSAR)

Geometry

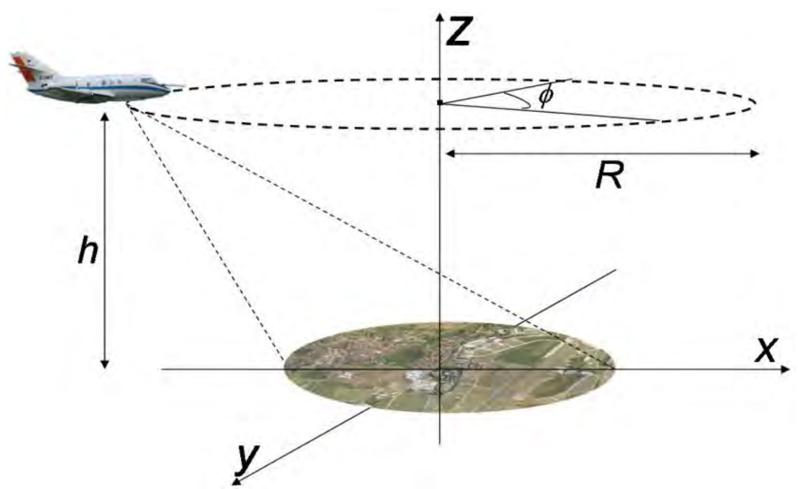

Super high resolution of $\lambda/4$

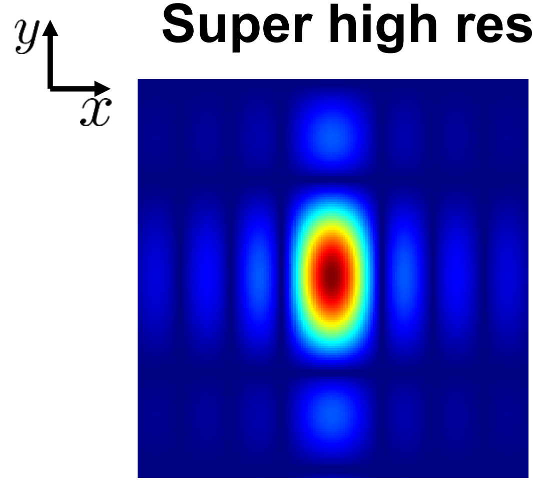

2-D IRF Stripmap

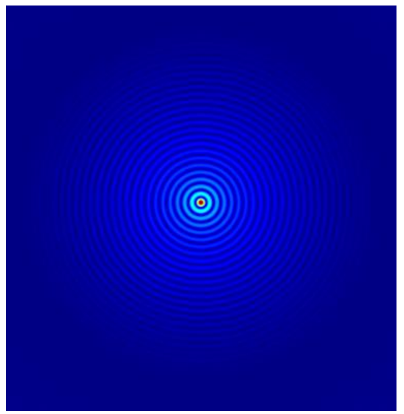

2-D IRF CSAR

3-D Reconstruction

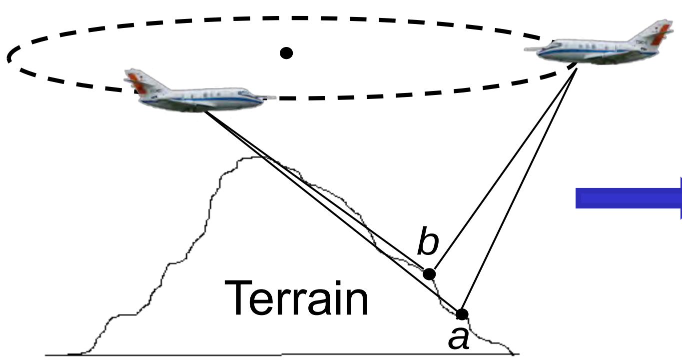

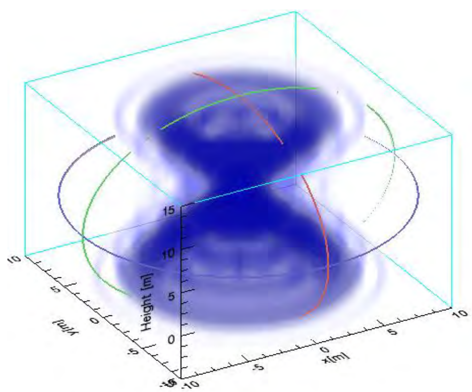

3-D IRF CSAR

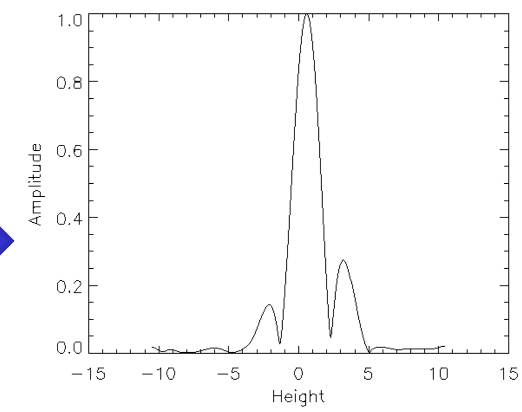

Height Profile

CSAR vs Strimap SAR

E-SAR L-band, 94MHz bandwidth

1500m x 1500m

Deutsches Zentrum für Luft- und Raumfahrt e.V. in der Helmholtz-Gemeinschaft

Courtesy of Octavio Ponce

Future Developments:

High Resolution Wide Swath (HRWS) Imaging

Development of new SAR Techniques: Motivation

State of the Art: TerraSAR-X	Imaging Mode		
	ScanSAR	Stripmap	Spotlight
Resolution	16 m	3 m	1 m
Swath Width	100 km	30 km	10 km

Resolution ⟷ Swath Width ⟷ Repeat Cycle

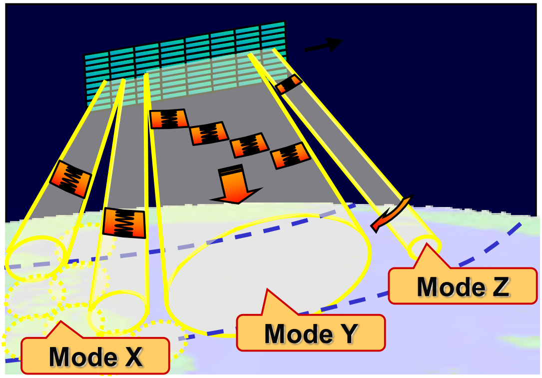

Future Requirements	Imaging Mode		
	Mode X	Mode Y	Mode Z
Resolution	5 m	1 m	<< 1 m
Swath Width	400 km	100 km	30 km

Limitation of Conventional SAR

- ➢ Unambiguous swath width and high azimuth resolution:
- → Contradicting requirements in SAR system design

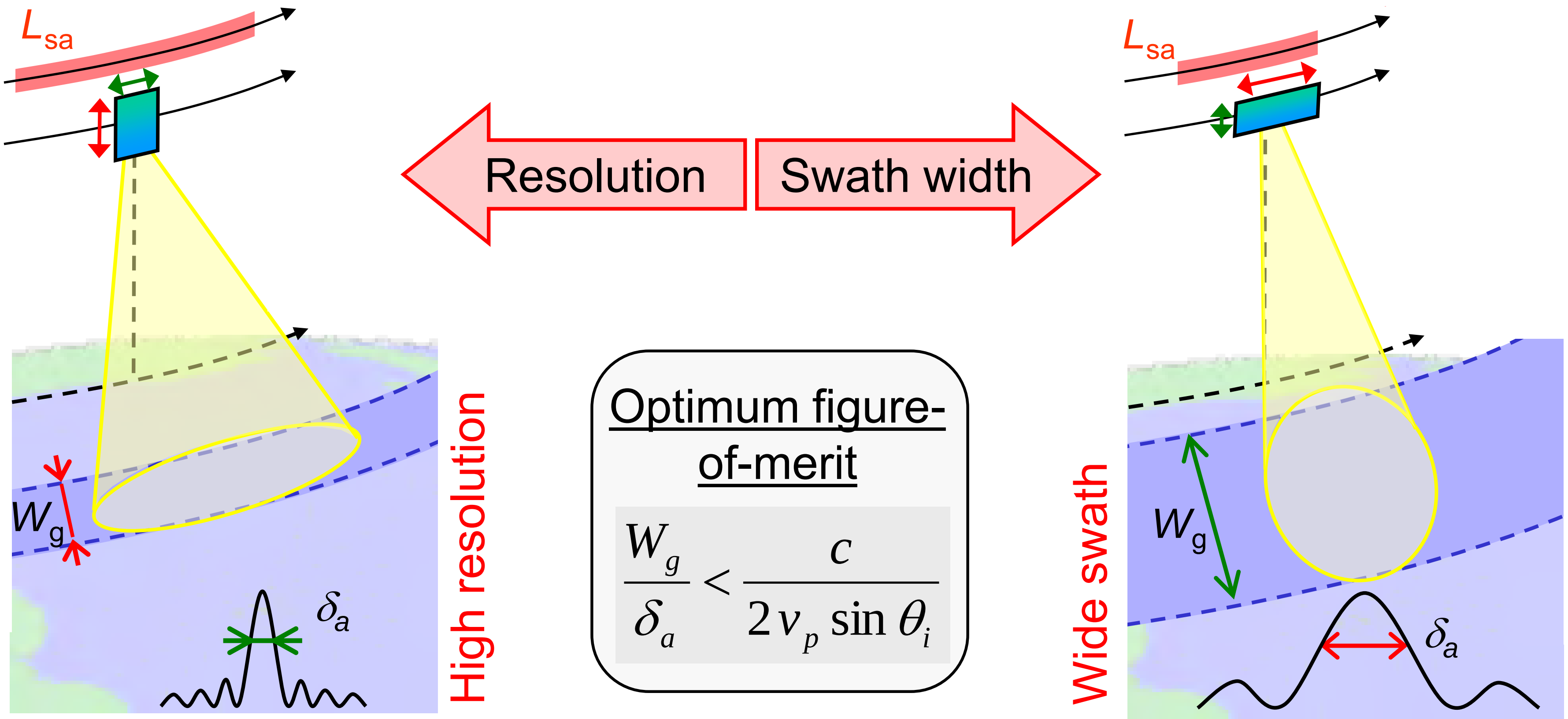

Optimum figure-of-merit

$$\frac{W_g}{\delta_a} < \frac{c}{2 v_p \sin\theta_i}$$

short antenna (azimuth) ⇒ high PRF (Nyquist) ⇒ **decreased swath width**

low antenna height (elevation) ⇒ low PRF (range ambiguities) ⇒ **worse azimuth res.**

New SAR Techniques: Digital Beamforming

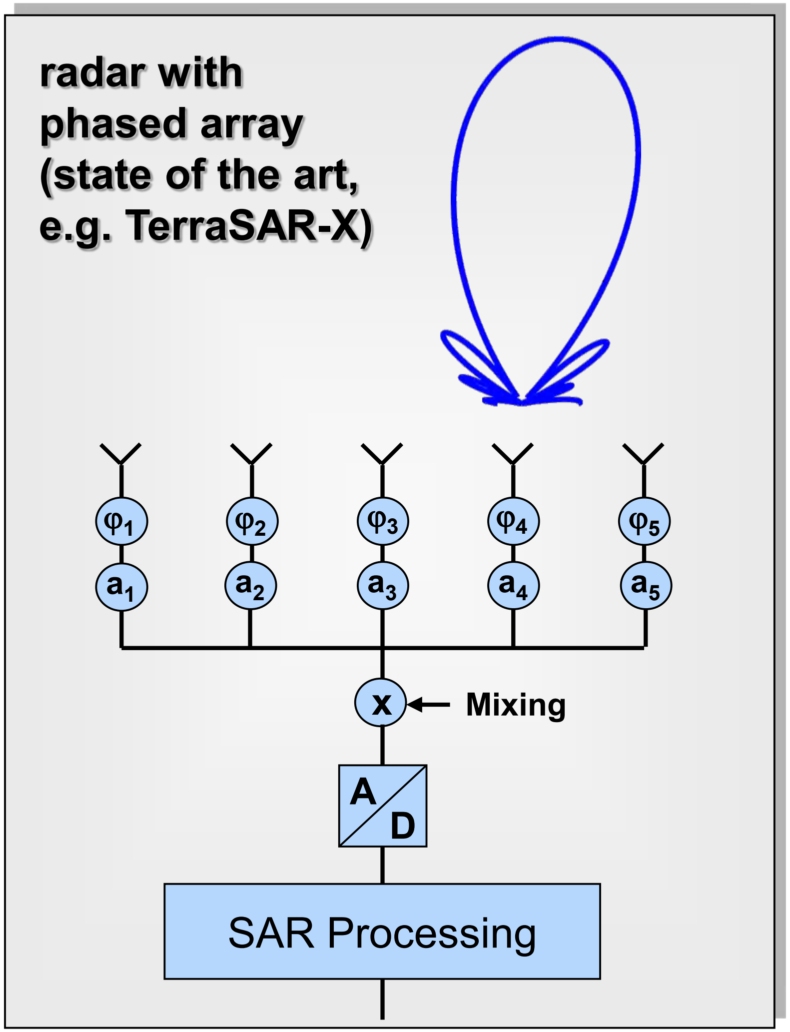

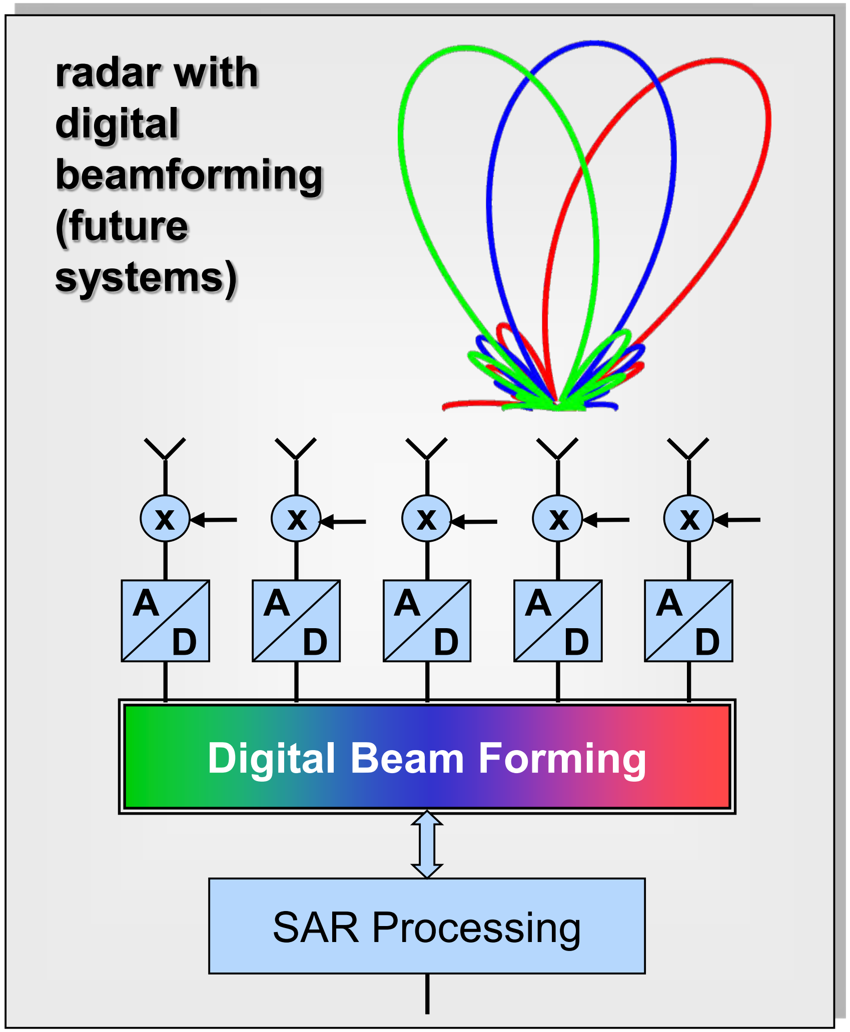

(Courtesy of G. Krieger)

Deutsches Zentrum für Luft- und Raumfahrt e.V. in der Helmholtz-Gemeinschaft

Wide Area Illumination

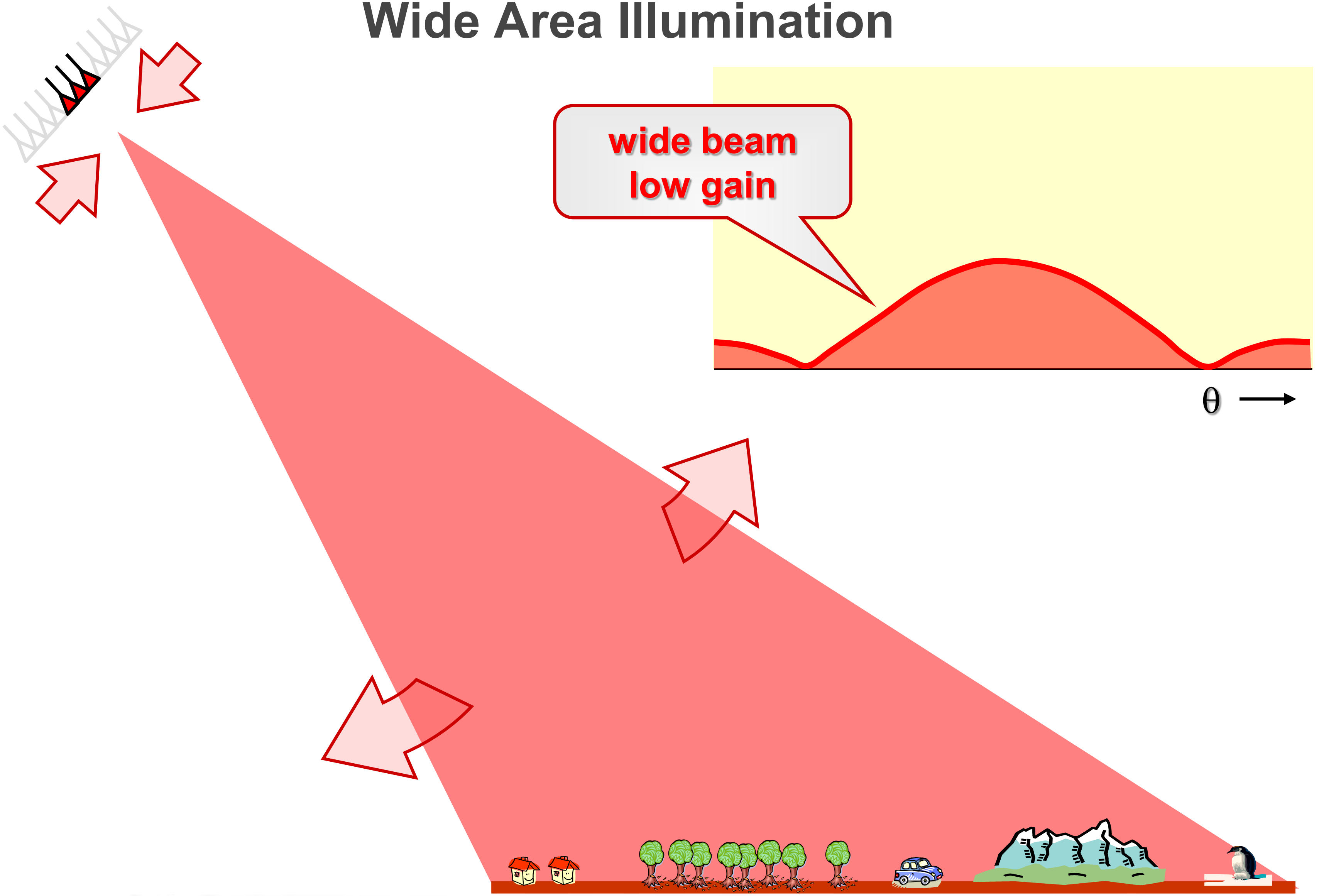

(Courtesy of G. Krieger)

Digital Beamforming on Receive

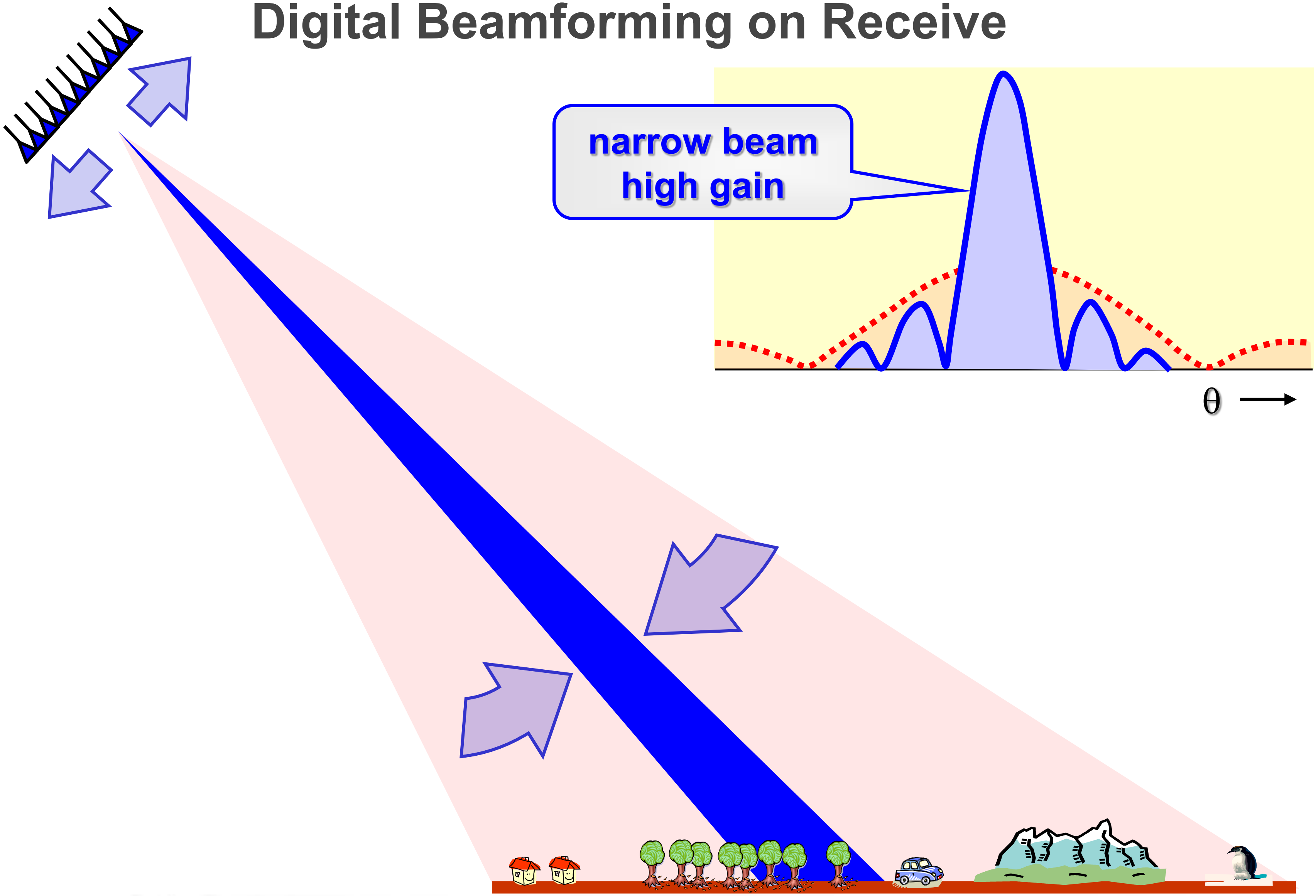

(Courtesy of G. Krieger)

Digital Beamforming on Receive

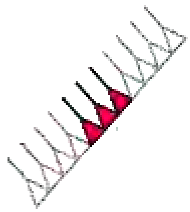

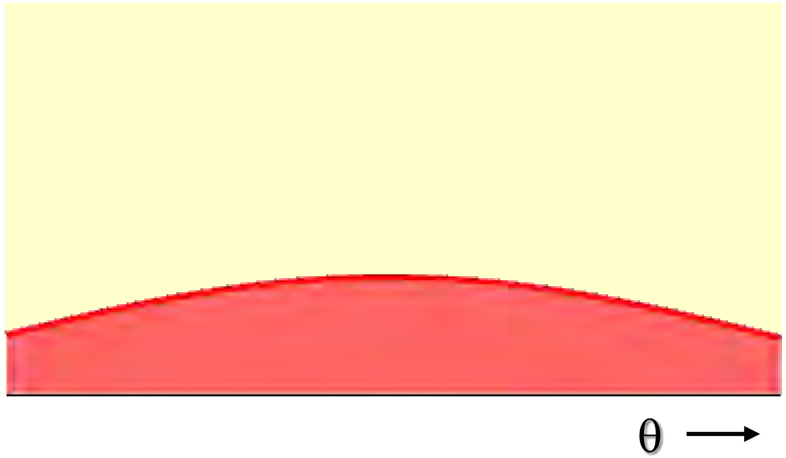

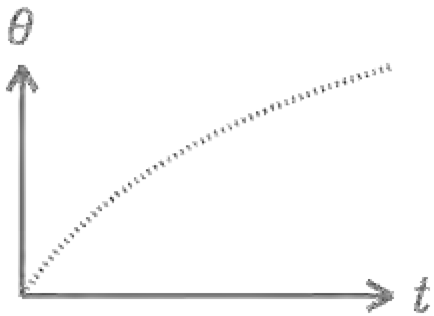

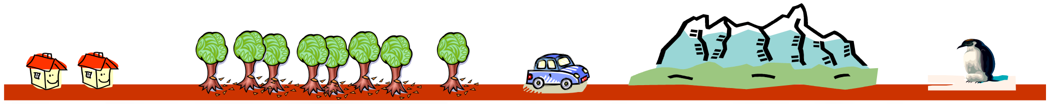

(Courtesy of G. Krieger)

Deutsches Zentrum für Luft- und Raumfahrt e.V. in der Helmholtz-Gemeinschaft

Digital Beamforming on Receive

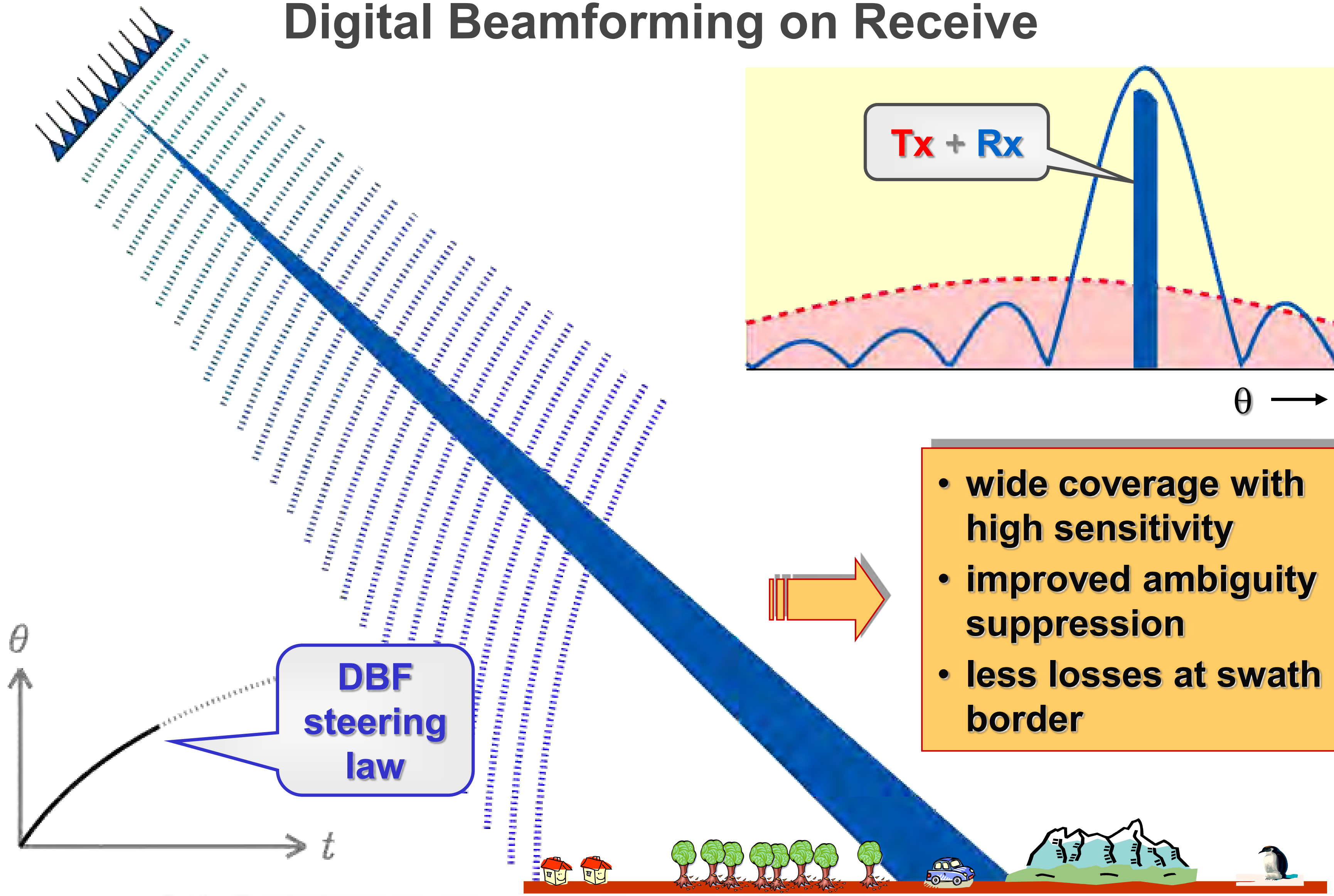

- wide coverage with high sensitivity
- improved ambiguity suppression
- less losses at swath border

(Courtesy of G. Krieger)

Deutsches Zentrum
DLR für Luft- und Raumfahrt e.V.
in der Helmholtz-Gemeinschaft

Deployable Reflector Antennas

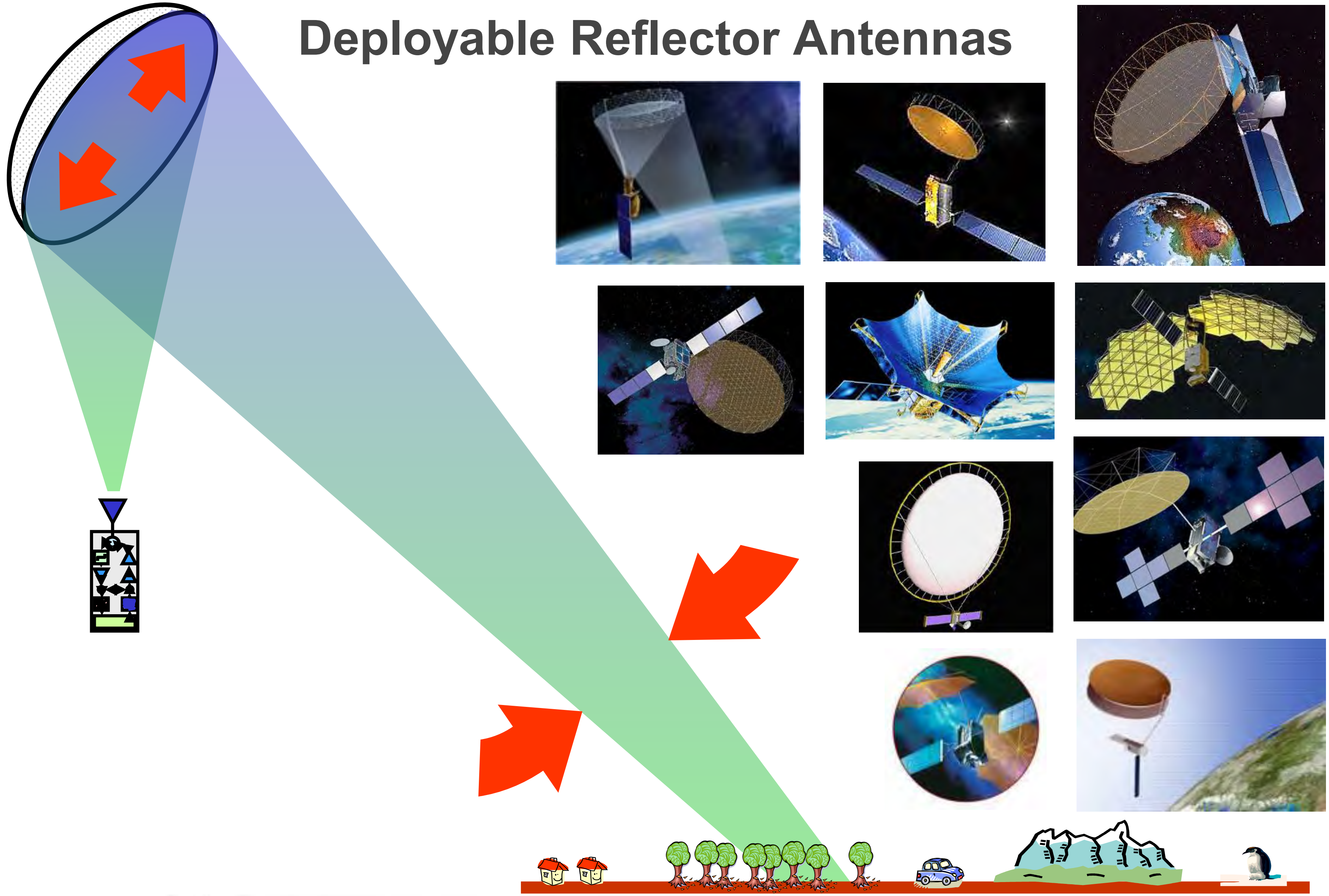

(Courtesy of G. Krieger)

DBF with Reflector Antennas

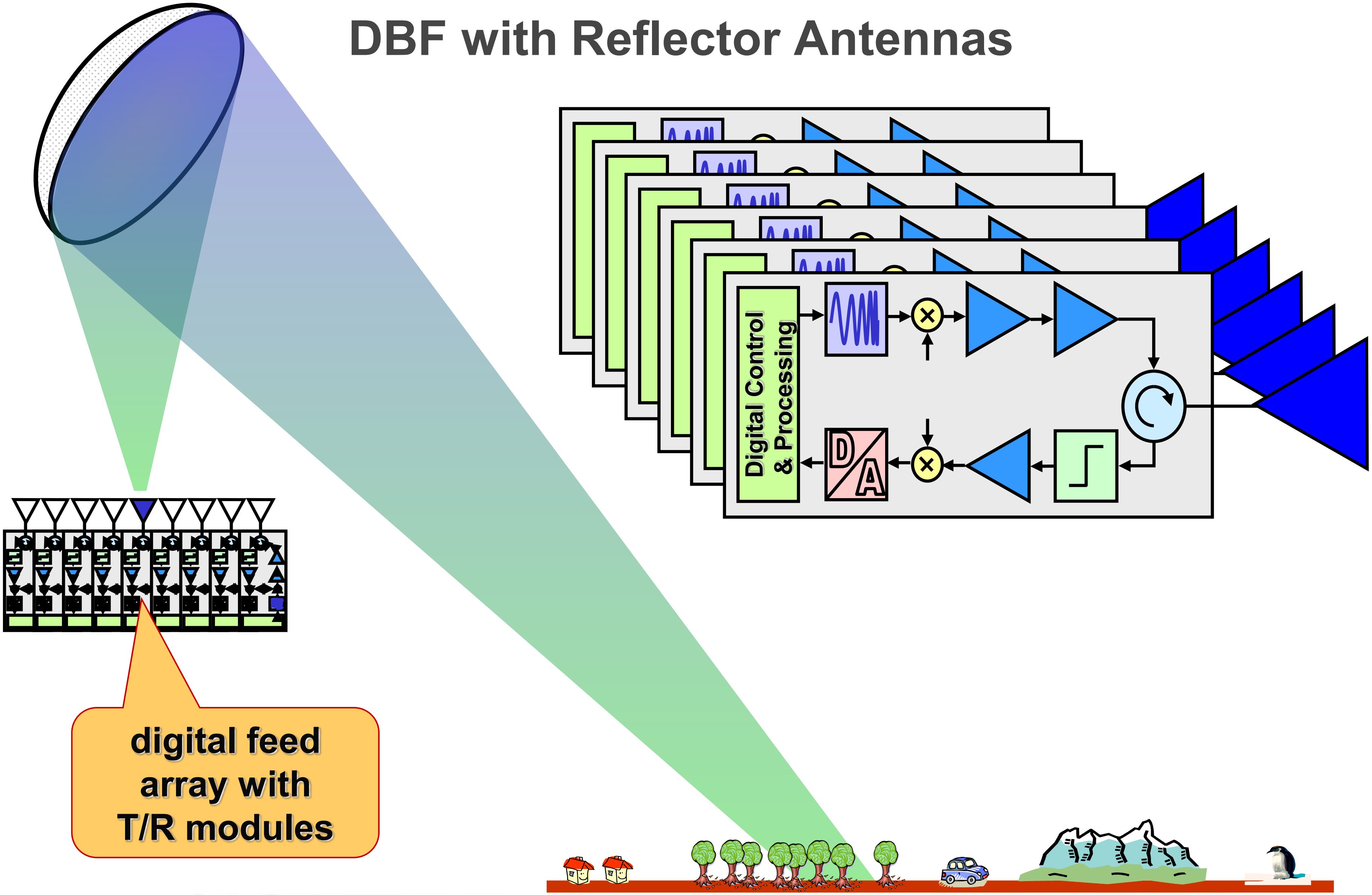

(Courtesy of G. Krieger)

DBF with Reflector Antennas

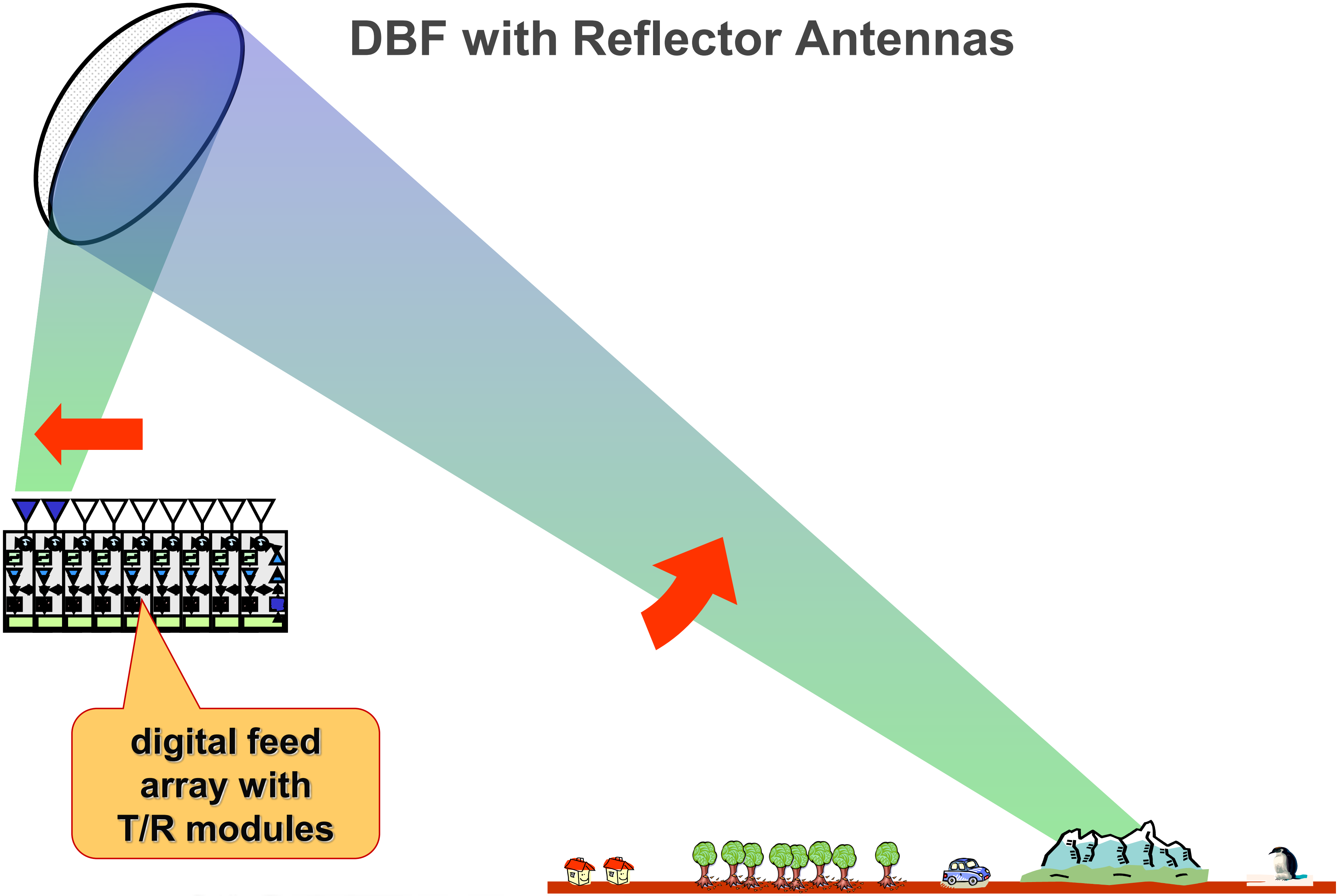

(Courtesy of G. Krieger)

DBF with Reflector Antennas

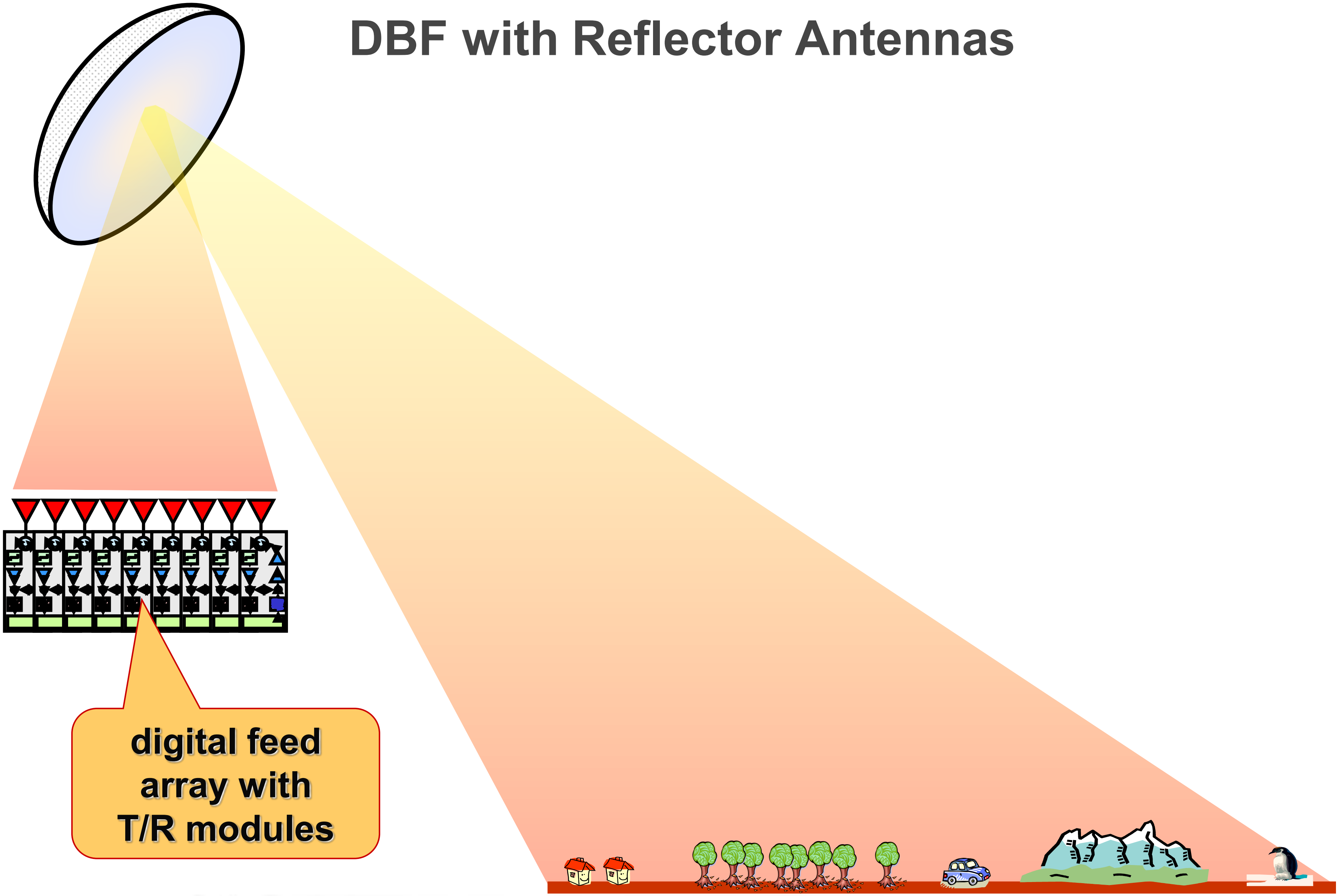

(Courtesy of G. Krieger)

DBF-SAR with Reflector Antennas

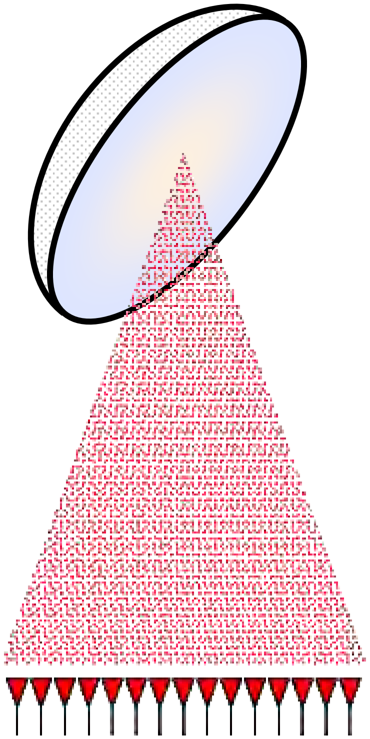

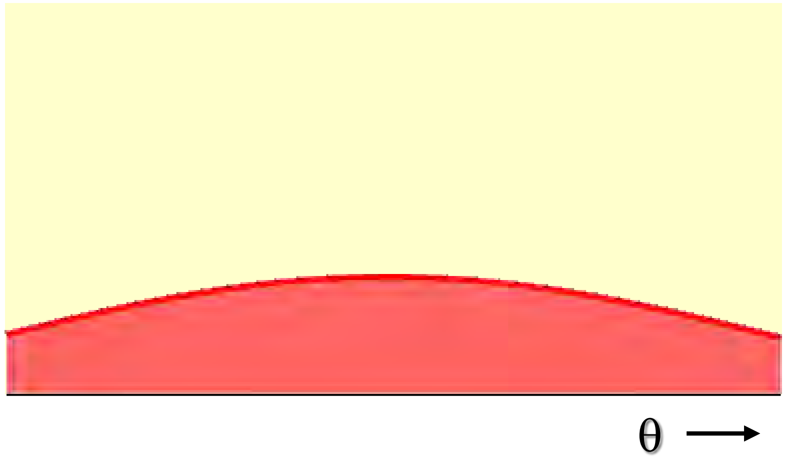

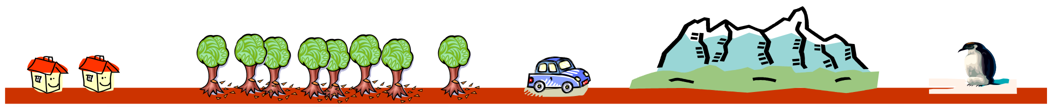

(Courtesy of G. Krieger)

DBF-SAR with Reflector Antennas

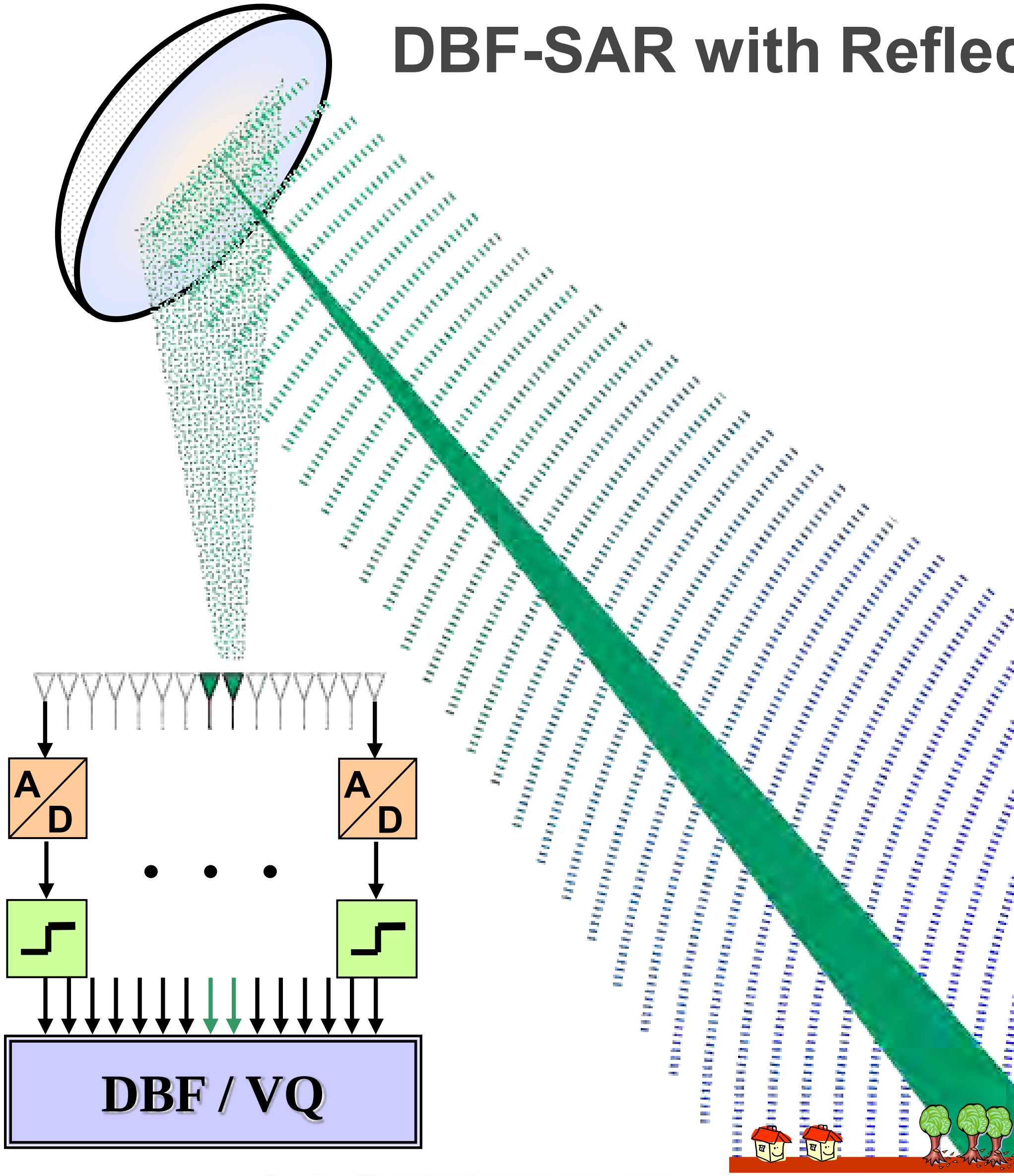

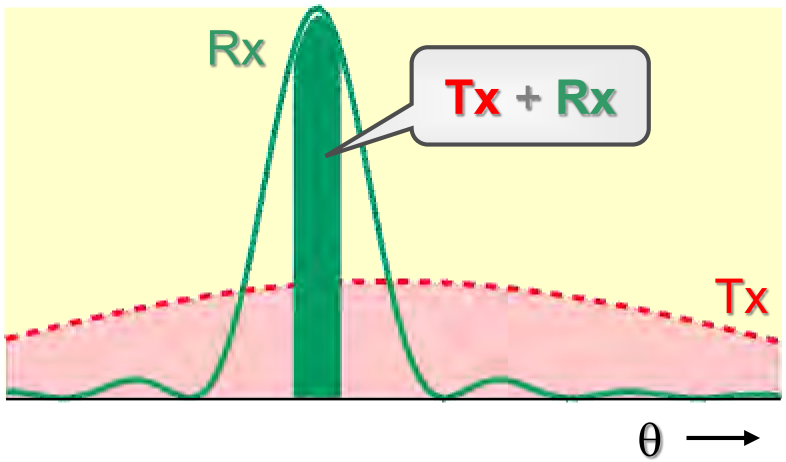

Large reflector enables:

- **high sensitivity also at low frequencies**
- **improved ambiguity suppression**
- **innovative SAR modes**
- **multiple frequency SAR**

(Courtesy of G. Krieger)

Potentials of Digital Radar

High Resolution and Coverage

- Suppression of interferences
- Increased sensivity
- Measurement of motions
- Resolving of ambiguities
- Adaptive & hybride SAR Modes
- …

Avoidance of User Conflicts

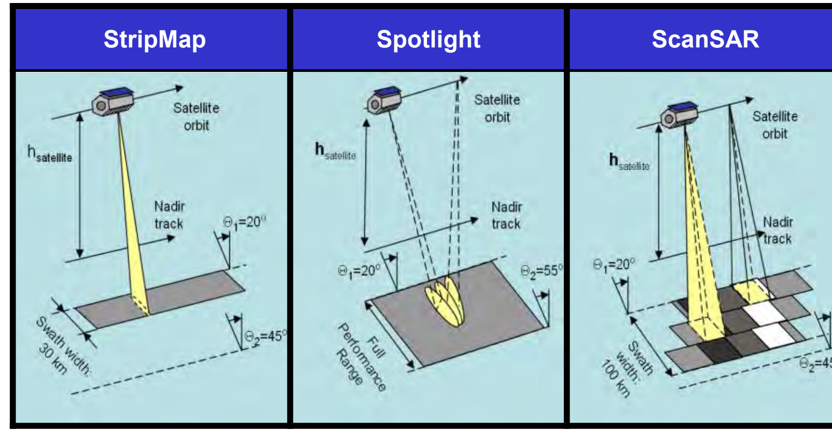

Frequent Observations

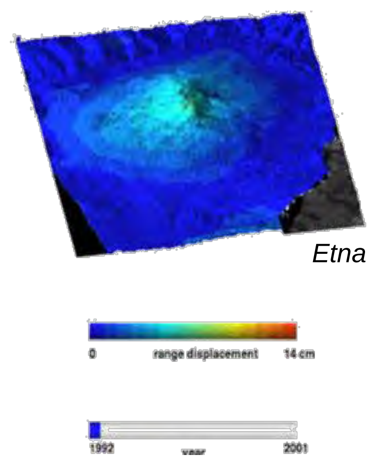

Etna

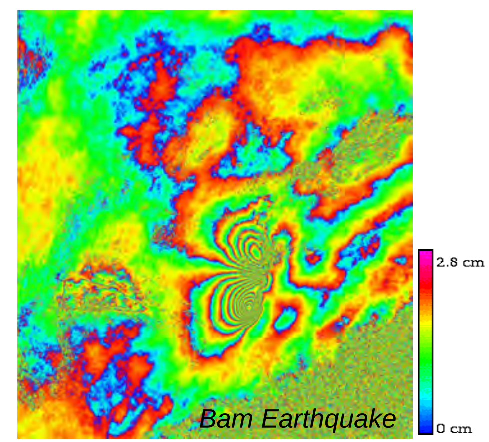

Bam Earthquake

Deutsches Zentrum für Luft- und Raumfahrt e.V. in der Helmholtz-Gemeinschaft

Potentials of Digital Radar

High Resolution and Coverage

Avoidance of User Conflicts

StripMap	Spotlight	ScanSAR

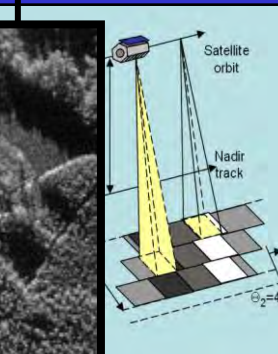

- Suppres
- Increase
- Measure
- Resolvi
- Adaptive
- ...

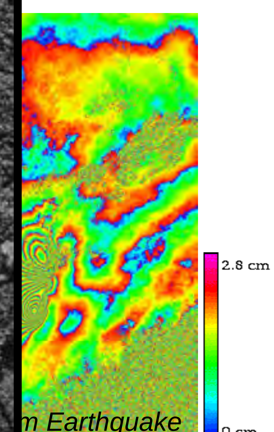

m Earthquake

in der Helmholtz-Gemeinschaft

Potentials of Digital Radar

High Resolution and Coverage

- Suppression of interferences
- Increased sensivity
- Measurement of motions
- Resolving of ambiguities
- Adaptive & hybride SAR Modes
- …

Avoidance of User Conflicts

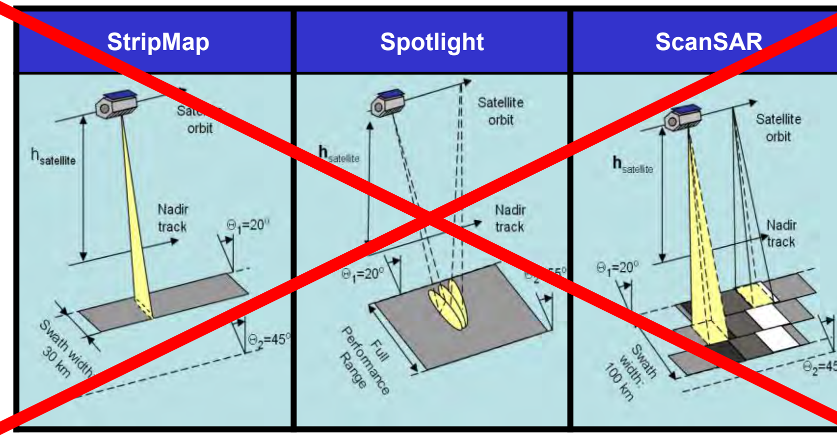

Frequent Observations

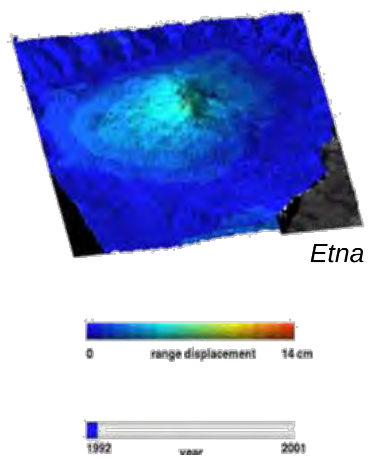

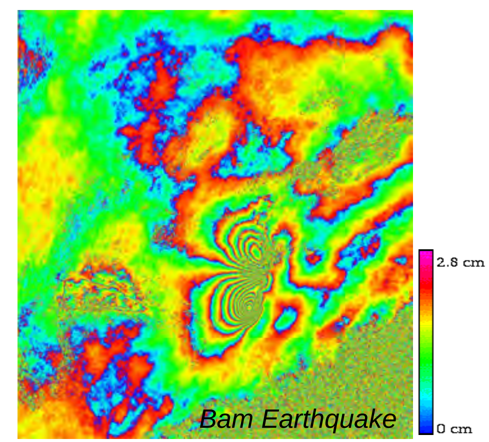

TanDEM-X

1 global acquisition / year

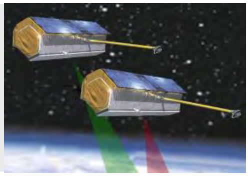

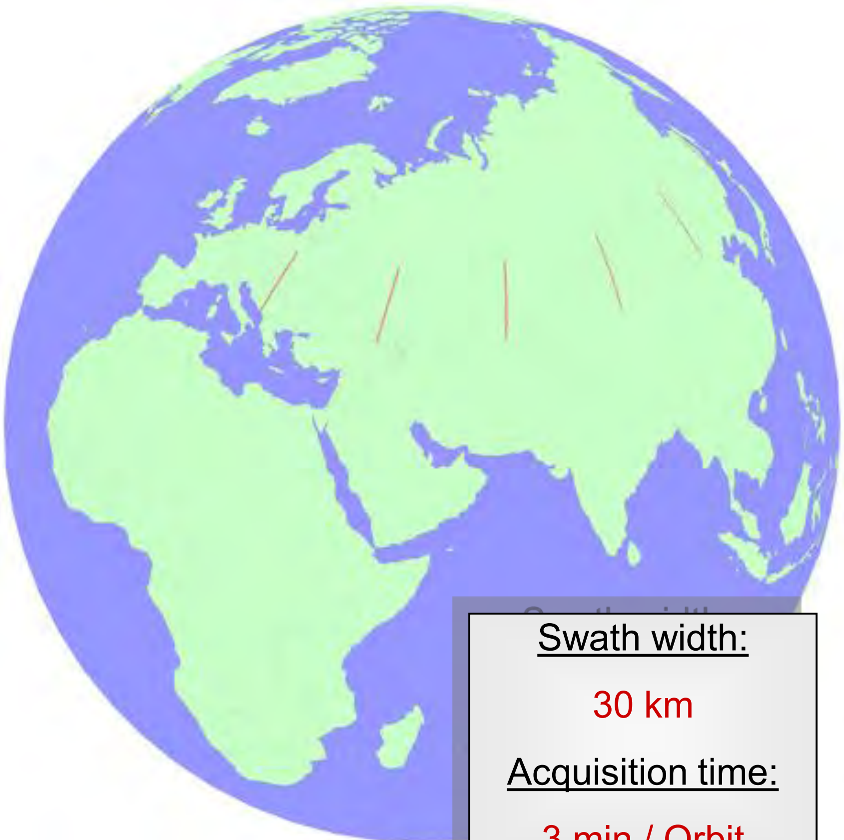

Swath width:

30 km

Acquisition time:

3 min / Orbit

Day

1

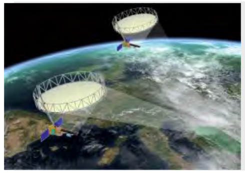

Tandem-L

2 global acquisitions / week

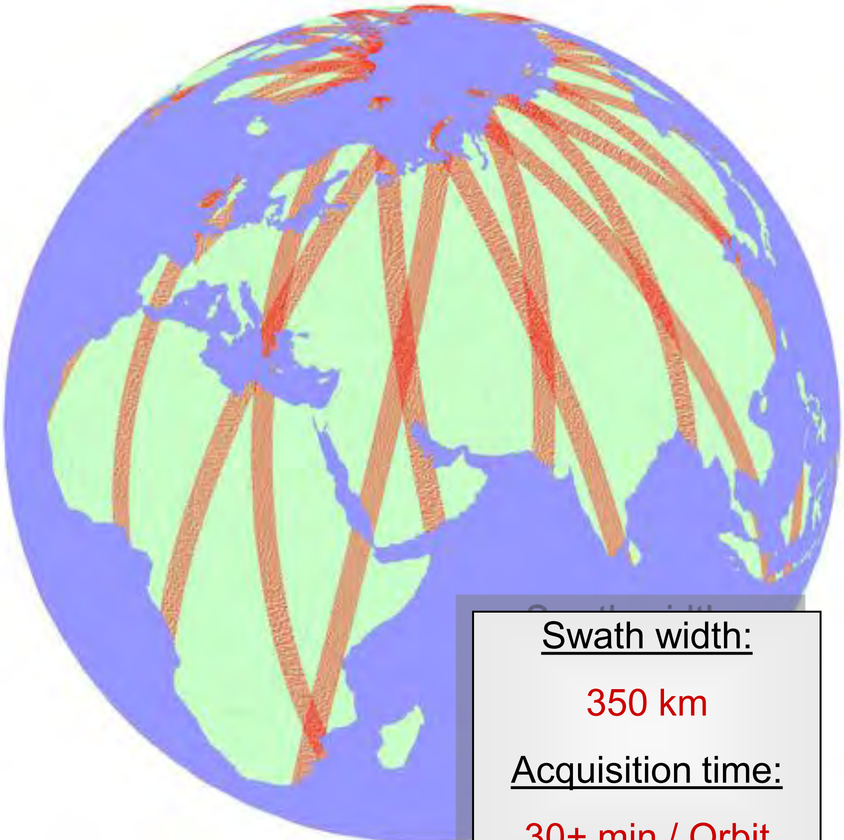

Swath width:

350 km

Acquisition time:

30+ min / Orbit

Many disciplines could be served by Tandem-L

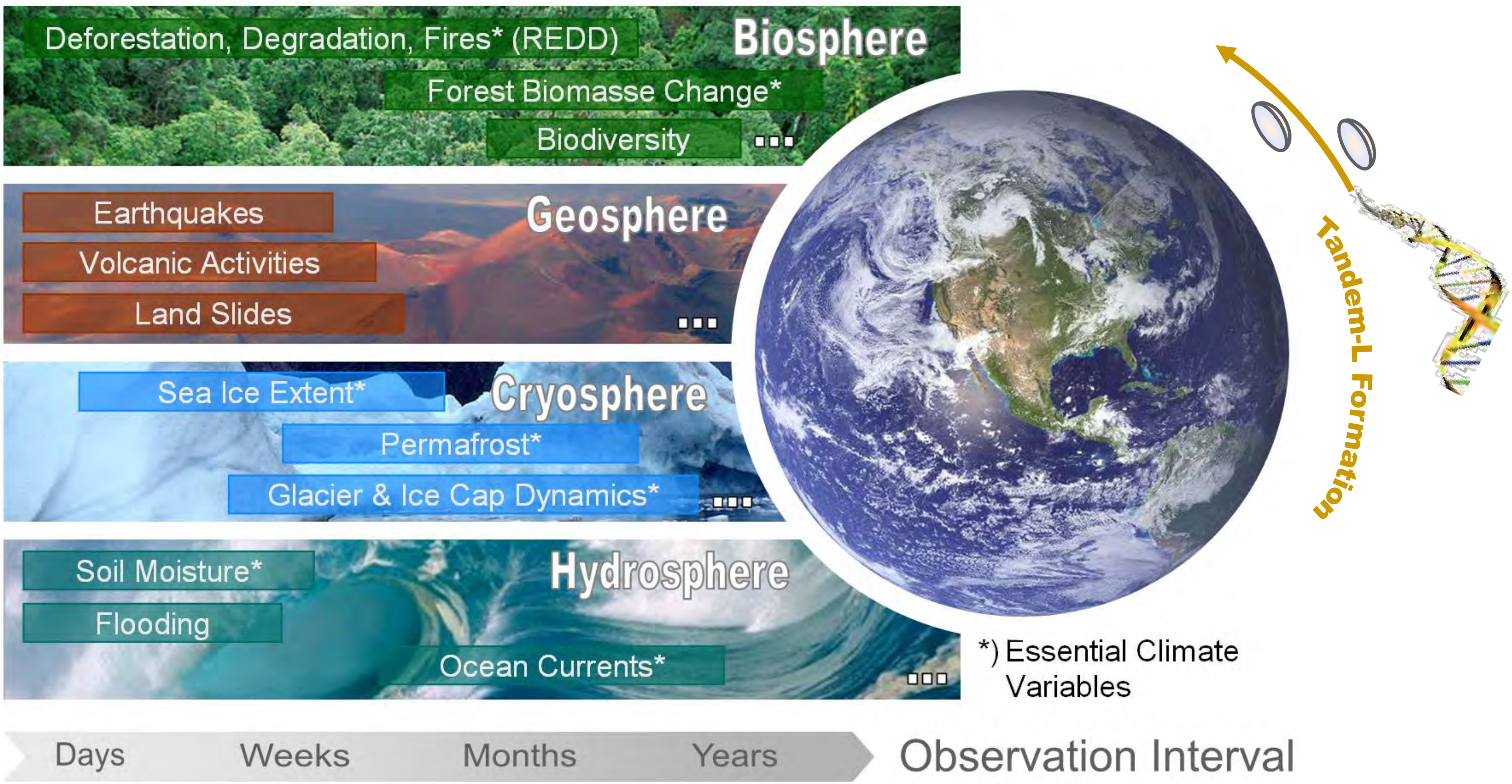

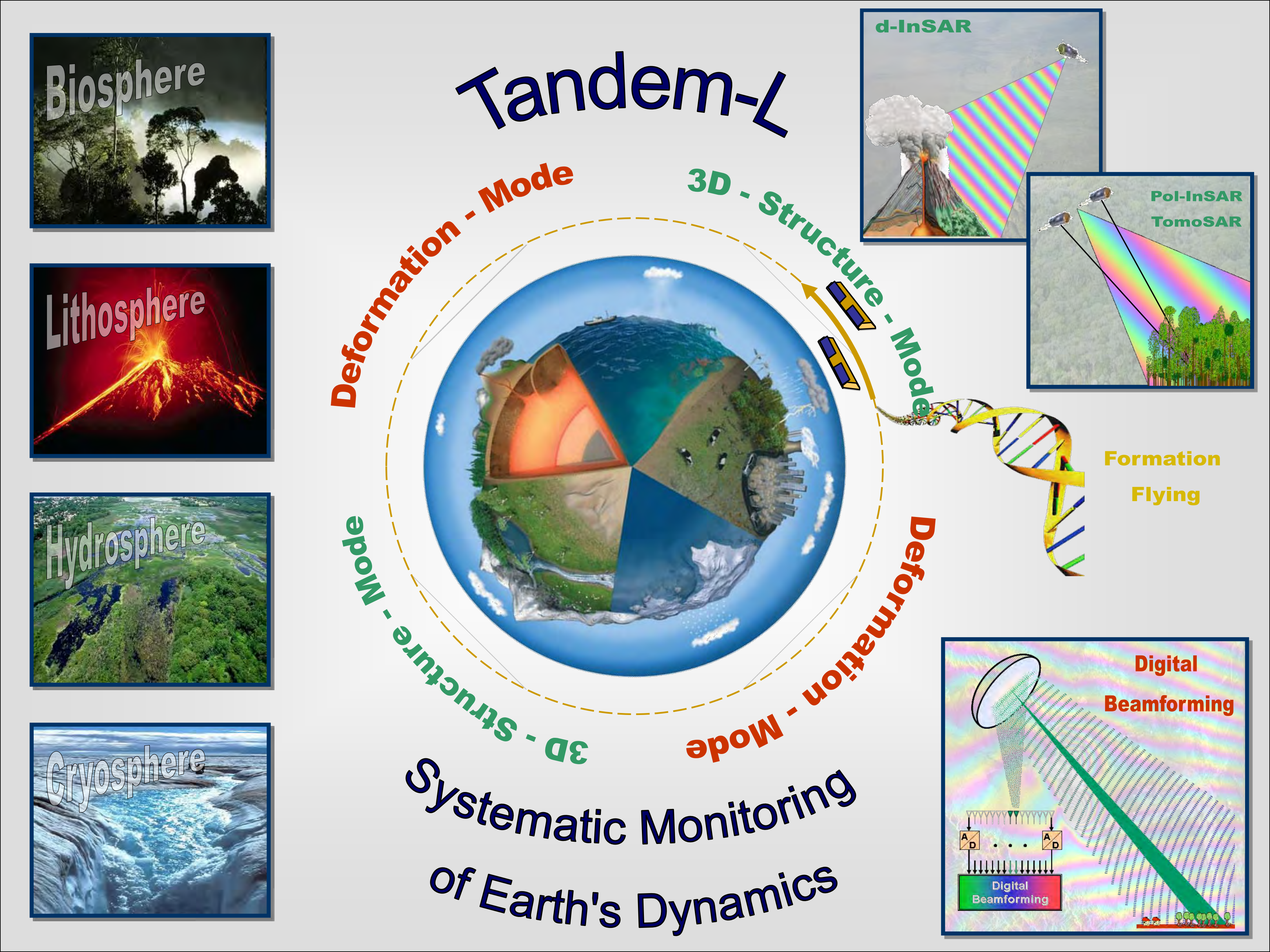
Tandem-L
Biosphere
Lithosphere
Hydrosphere
Cryosphere
Deformation - Mode
3D - Structure - Mode
Deformation - Mode
3D - Structure - Mode
d-InSAR
Pol-InSAR
TomoSAR
Formation
Flying
Digital
Beamforming
A D
A D
Digital
Beamforming
Systematic Monitoring
of Earth's Dynamics

New Mission Proposals: Additional Concepts and Analysis

Radarsystems With Passive Receivers

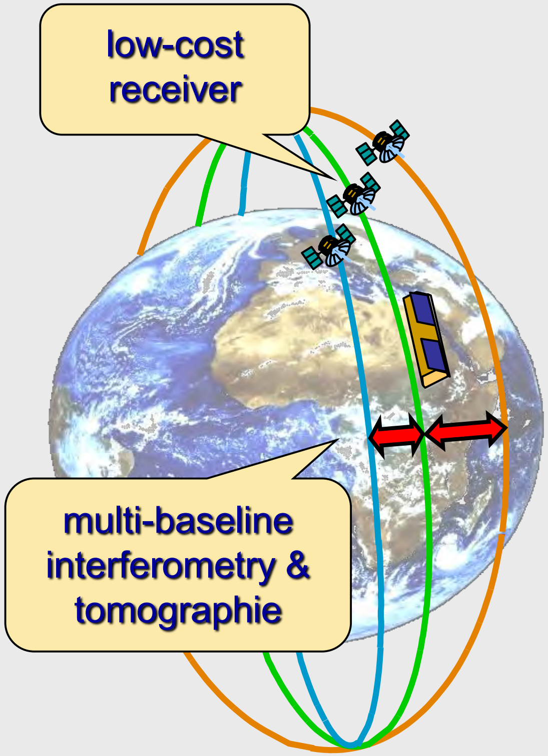

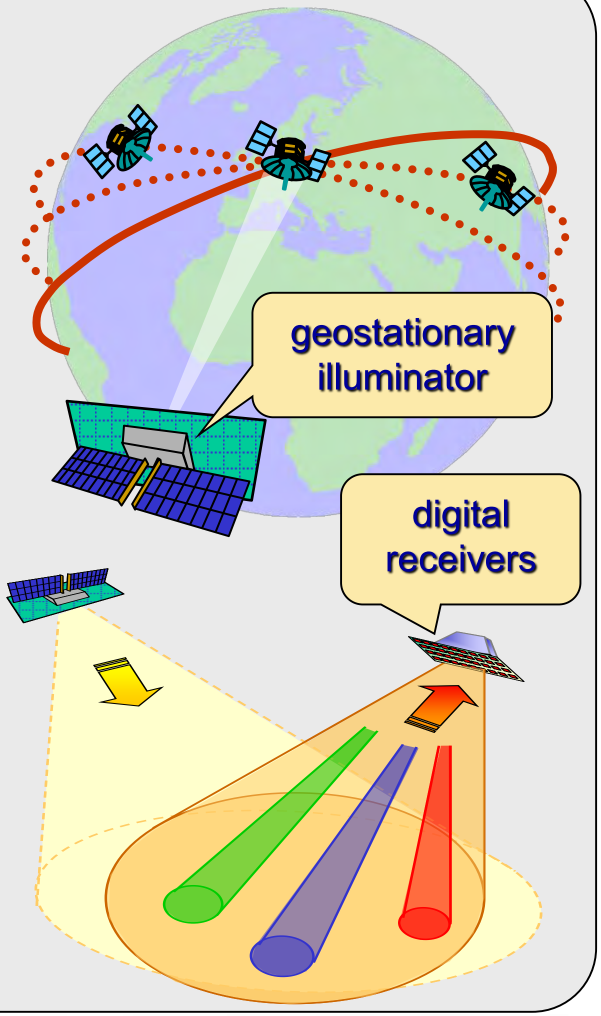

Moon Radar

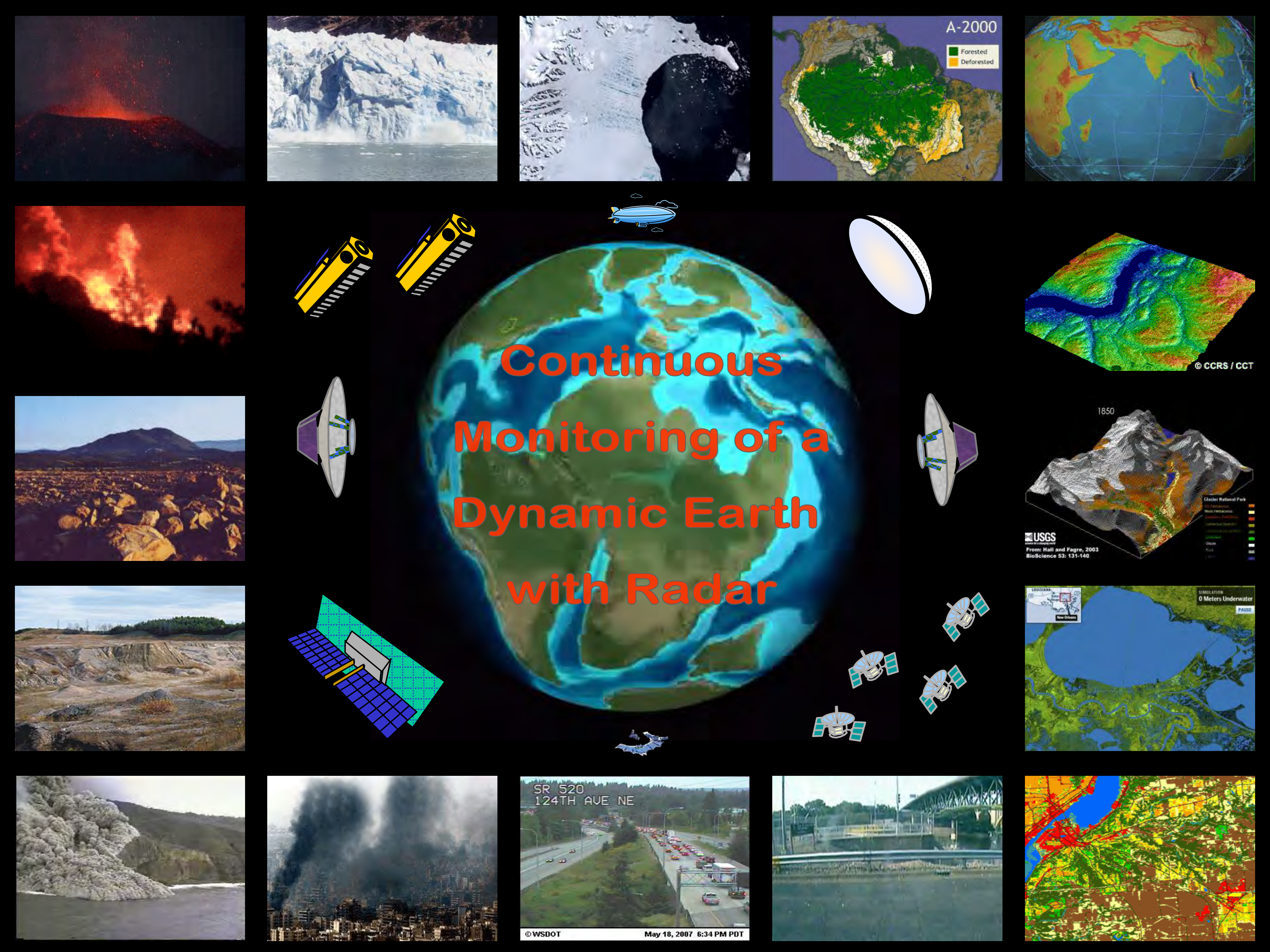
A-2000
Forested
Deforested
© CCRS / CCT
Continuous Monitoring of a Dynamic Earth with Radar
1850
USGS
From: Hall and Fagre, 2003
BioScience 53: 131-140
Glacier National Park
0 Meters Underwater
PAUSE
SR 520
124TH AVE NE
©WSDOT
May 18, 2007 6:34 PM PDT

Thanks for your attention!

References

- **SAR Basics and Processing:**
  - J. C. Curlander, R. N. McDonough, Synthetic Aperture Radar: Systems and Signal Processing. New York: Jon Wiley & Sons, 1991.
  - I. Cumming, F. Wong, Digital processing of synthetic aperture radar data: signal processing algorithms. Boston: Artech House, 2005.
  - F. Henderson (Ed.), Manual of Remote Sensing: Principles and Applications of Radar Imaging, Wiley, 1999.
- **Interferometry, Polarimetric SAR Interferometry, Tomography**
  - R. Hanssen, Radar interferometry: data interpretation and error analysis, Dordrecht, Kluwer Academic Publishers, 2001.
  - K. Papathanassiou, S. Cloude, “Single-baseline polarimetric SAR interferometry”, IEEE Transactions on Geoscience and Remote Sensing, Vol. 39, No. 11, pp. 2352-2363, 2001.
  - A. Reigber, A. Moreira, “First demonstration of airborne SAR tomography using multibaseline L-band data”, IEEE Trans. Geosc. and Remote Sens., Vol. 38, No. 5, pp. 2142-2152, 2000.
- **SRTM, TerraSAR-X, TanDEM-X**
  - T. Farr et al. "The Shuttle Radar Topography Mission", Reviews of Geophysics, vol. 45, 2007.
  - M. Stangl, R. Werninghaus, B. Schweizer, C. Fischer, M. Brandfass, J. Mittermayer, H. Breit, "TerraSAR-X technologies and first results", IEE Proceedings - Radar, Sonar and Navigation, vol. 153, pp. 86-95, 2006.
  - G. Krieger, A. Moreira, H. Fiedler, I. Hajnsek, M. Younis, C. Werner, and M. Zink, "The TanDEM-X mission: a satellite formation for high resolution SAR interferometry", to appear in IEEE Transactions on Geoscience and Remote Sensing, 2007.

References

- **Bistatic and Multistatic SAR**
  - N. Willis, Bistatic radar, Artech House, Boston, 1991.
  - A. Moccia, N. Chiacchio, A. Capone, “Spaceborne bistatic synthetic aperture radar for remote sensing applications”, Int. J. Remote Sens., Vol. 21, No. 18, pp. 3395-3414, 2000.
  - P. Dubois-Fernandez, H. Cantalloube, B. Vaizan, G. Krieger, R. Horn, M. Wendler, and V. Giroux, "ONERA-DLR bistatic SAR campaign: Planning, data acquisition, and first analysis of bistatic scattering behavior of natural and urban targets", IEE Proc. - Radar, Sonar, Navigation, vol. 153, pp. 214-223, 2006.
  - G. Krieger, A. Moreira, “Spaceborne bi- and multistatic synthetic aperture SAR: potential and challenges”, IEE Proceedings on Radar Sonar and Navigation, vol. 153, pp. 184-198, 2006.
  - M. Cherniakov (editor), Bistatic radars: emerging technology (2 volumes), John Wiley & Sons, 2007.
- **High Resolution Wide Swath Imaging and Digital Beamforming SAR**
  - A. Currie and M. A. Brown, "Wide-swath SAR", IEE Proceedings F - Radar and Signal Processing, vol. 139, pp. 122-135, 1992.
  - G. D. Callaghan and I. D. Longstaff, "Wide-swath space-borne SAR using a quad-element array", Radar, Sonar and Navigation, IEE Proceedings - Radar, Sonar, Navigation, vol. 146, pp. 159-165, 1999.
  - M. Suess, B. Grafmueller, and R. Zahn, "A novel high resolution, wide swath SAR system", in Proc. IEEE Geoscience and Remote Sensing Symposium, Sydney, Australia, pp. 1013-1015, 2001.
  - G. Krieger, N. Gebert, A. Moreira, “Multidimensional Waveform Encoding: A New Digital Beamforming Technique for Synthetic Aperture Radar Remote Sensing”, to appear in IEEE Transactions on Geoscience and Remote Sensing, 2007.

Airborne SAR Systems

AES1

AeroSensing (D)

GulfStream Commander

X-Band (HH), P-Band (Quad)

AIRSAR

NASA / JPL (USA)

DC8

P, L, C-Band (Quad)

DOSAR

EADS / Dornier GmbH (D)

DO 228 (1989), C160 (1998), G222 (2000)

S, C, X-Band (Quad), Ka-Band (VV)

RENE

UVSQ / CETP (F)

Écureuil AS350

S, X-Band (Quad)

E-SAR

DLR (D)

DO 228

P, L, S-Band (Quad)

C, X-Band (dual)

EMISAR

DCRS (DK)

G3 Aircraft

L, C-Band (Quad)

AER II-PAMIR

FGAN (D)

Transal C160

Ka, W-Band (Quad) / X-Band (Quad)

STORM

UVSQ / CETP (F)

Merlin IV

C-Band (Quad)

PHARUS

TNO - FEL (NL)

CESSNA – Citation II

C-Band (Quad)

PISAR

NASDA / CRL (J)

GulfStream

L, X-Band (Quad)

RAMSES

ONERA (F)

Transal C160

P, L, S, C, X, Ku, Ka, W-Band (Quad)

SAR580

CCRS (CA)

Convair CV-580

C, X-Band (Quad)

E-SAR on Bord the Do-228

- Flexible multi-channel SAR-system
- Frequency bands: X, C, S, L and P
- Fully-polarimetric in L- and P-band

<u>Typical flight geometry</u>

- flight altitude: 3000 m above ground
- flight speed: 90 m/s
- cruising range: 3 h (ca. 2.5 h measurement)
- sensor weight: 700 kg
- no. of operators: 2

- Dual-polarimetric in C-band
- interferometric in X-Band
- azimuth resolution up to 0.2 m
- innovative imaging modes

F-SAR Concept

- Successor of DLR's E-SAR
- Multi-functional SAR system
- Multi-spectral & fully polarimetric in X-, C-, S-, L- and P-band
- Range bandwidth 800 MHz
- Currently: PRF_{max} = 5 kHz
- Incidence angle 25 .. 60°
- Altitude up to 6000 MSL
- Development is ongoing

DO228-212


System Control
Data Acquisition


C-S-Band TX/RX


X-Band TX/RX
X-C-S Converter